Advanced Component Technology Program

JPL UCLA

Micro-Electro-Mechanical-Systems (MEMS) Actuated Wave Front Controller: Distortion Compensation for Inflatable Antennas

William A. Imbriale (1), Yahya Rahmat-Samii (2), Harish Rajagopalan (2), Shenheng Xu (2) and Vahraz Jamnejad (1)

(1) Jet Propulsion Laboratory, California Institute of Technology

(2) Department of Electrical Engineering, University of California, Los Angeles

June 24, 2008

ESTO Earth Science Technology Office

Motivation

- The Solid Earth Sciences Working Group (SESWG) specifically identifies lightweight antennas in the 14m, 20m and 30m class as one of the new technologies that will result in the highest science payoff
- The technology that can best provide large light-weight, low cost antennas is an inflatable structure technology
- The first 14m inflatable antenna that was deployed in space failed to meet its surface accuracy requirement
- The purpose of this task is to provide a technology that will significantly reduce the inflatable structure surface accuracy requirement by compensating for the surface errors in real time

Key Elements of the Task

- Provide a methodology for determining the main reflector distortion in real time
- Provide the design of a reconfigurable subreflector that will compensate for these distortions
  - The subreflector will consist of MEMS switches integrated with patch reflectarray elements
  - A representative sample will be fabricated and tested
- Provide the analysis to quantify the amount of compensation provided

MEMS Controlled Reflectarray Compensation Methodology

1. Certain distortions exist on the main reflector.

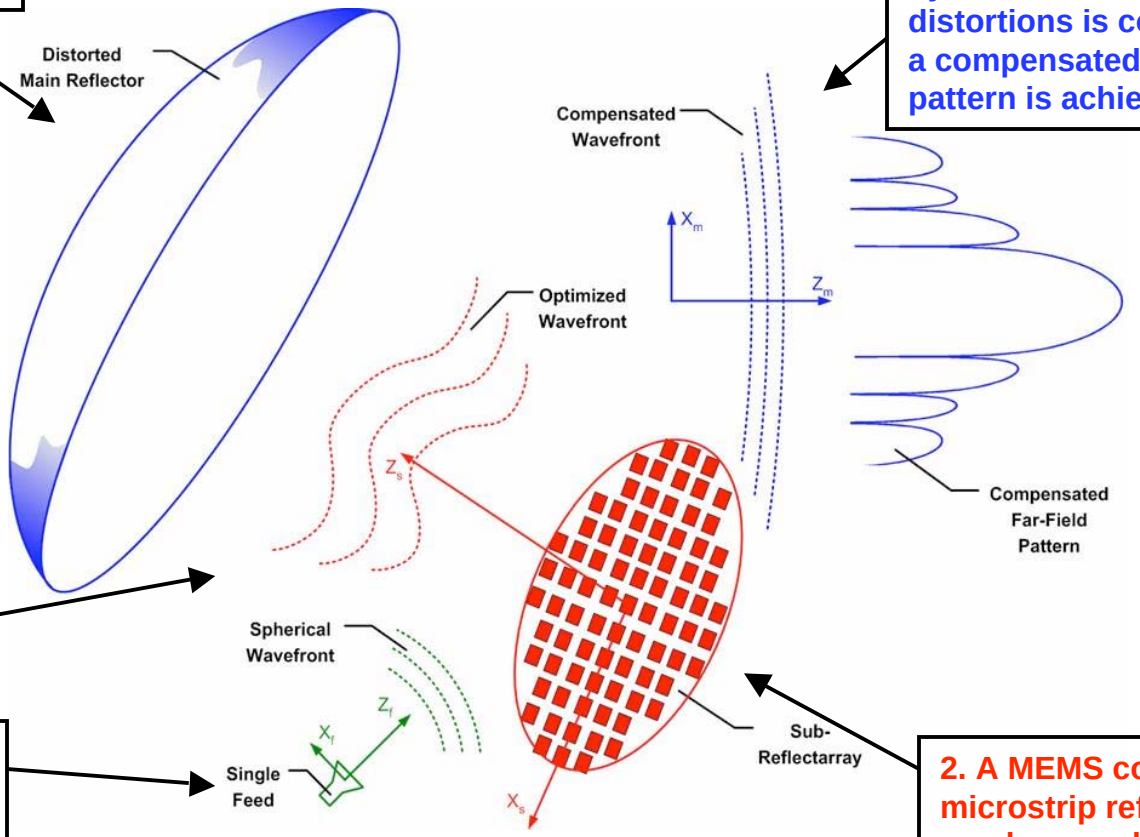

5. The phase error caused by the main reflector surface distortions is corrected, and a compensated far-field pattern is achieved.

4. By properly adjusting the reflection phase of each sub-reflectarray element, the re-radiated field is optimized.

3. The sub-reflectarray is illuminated by a primary feed.

2. A MEMS controlled microstrip reflectarray is used as a subreflector.

Advantages

- There are several significant and unique advantages to this approach
- Since the main reflector is measured in real time the following distortion sources are compensated
  - Manufacturing errors
  - Initial on-orbit deployment errors
  - Any long term changes in material properties
  - Thermal effects
- Since it uses MEMS switches
  - It is low cost
  - It is extremely lightweight
  - It has low power consumption
  - It has less RF loss than electronic switches

Outline

- Methodology for determining real time main reflector distortion
- Sub-reflectarray distortion compensation
- Selection of optimum patch reflectarray element
- Integration of MEMS into the reflectarray element
- Conclusions

Algorithms for main reflector surface determination

Three algorithms for main reflector surface determination were developed

- A two-camera optical surface-measuring system using photogrammetry
- A small array feed placed in the focal plane of the reflector system
- Small probes placed on the subreflector

– It was demonstrated that all three methods can recover the main reflector distortion

– The subreflector probe method seems to offer the simplest (least number of probes and minimal computation) implementation

- An Experiment is proposed to test and verify the subreflector probe method

Two camera photogrammetry

Measurements of thermal distortion made every 5 minutes

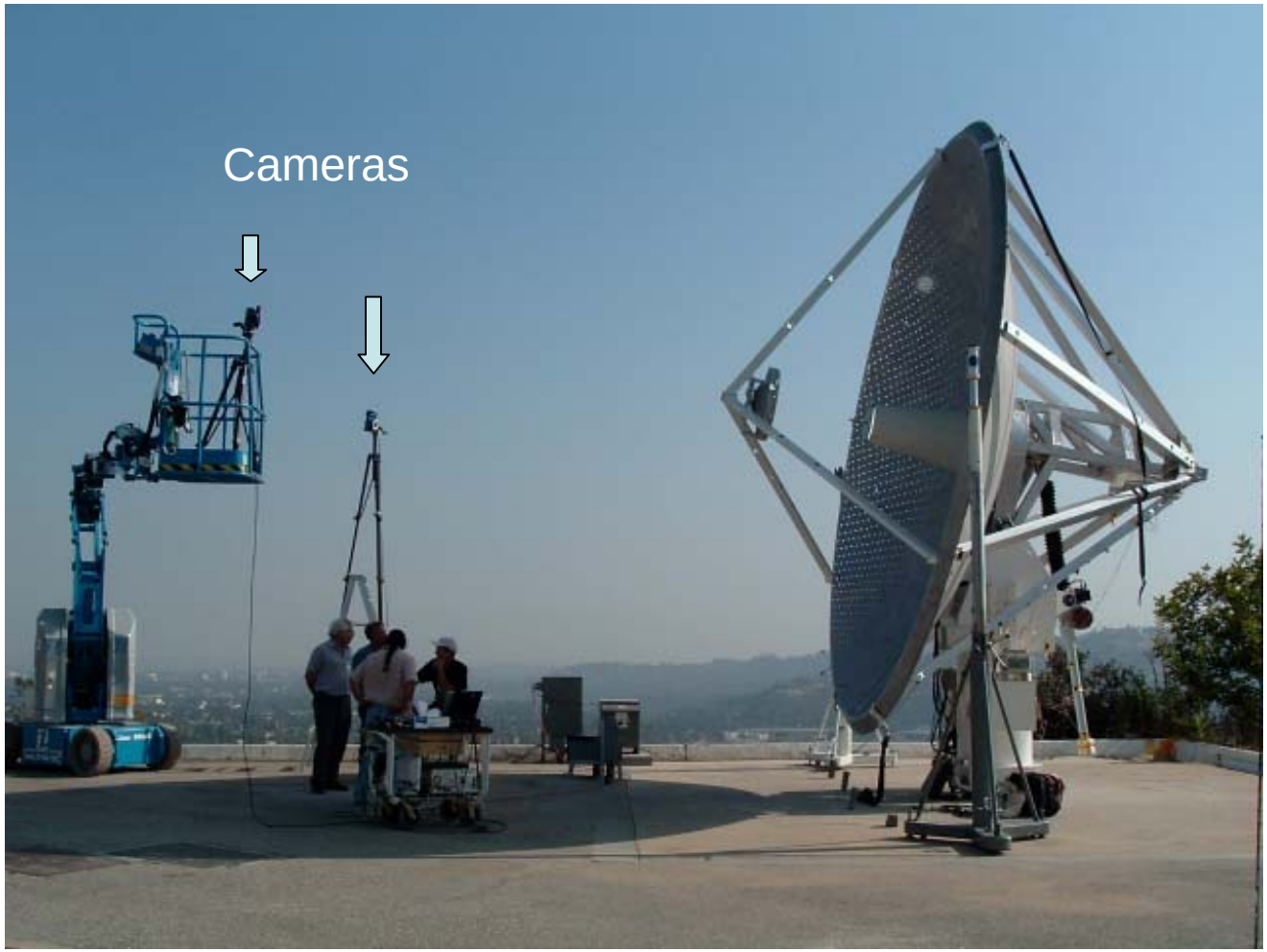

Points measured on reflector

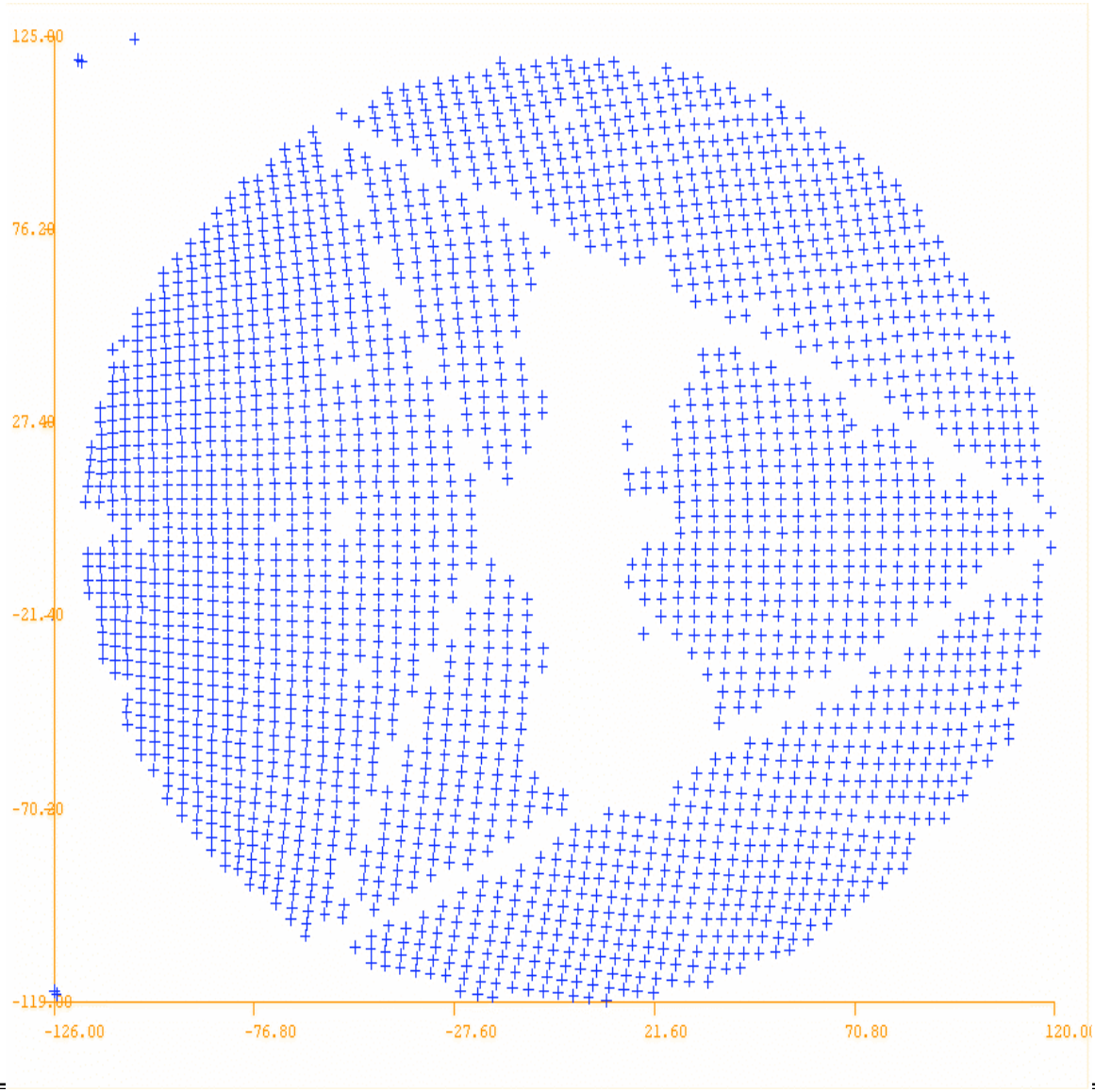

Top of reflector

An example of measured surface error

Discrete points RMS error = 23.8 mils

10 x 10 term Zernike representation

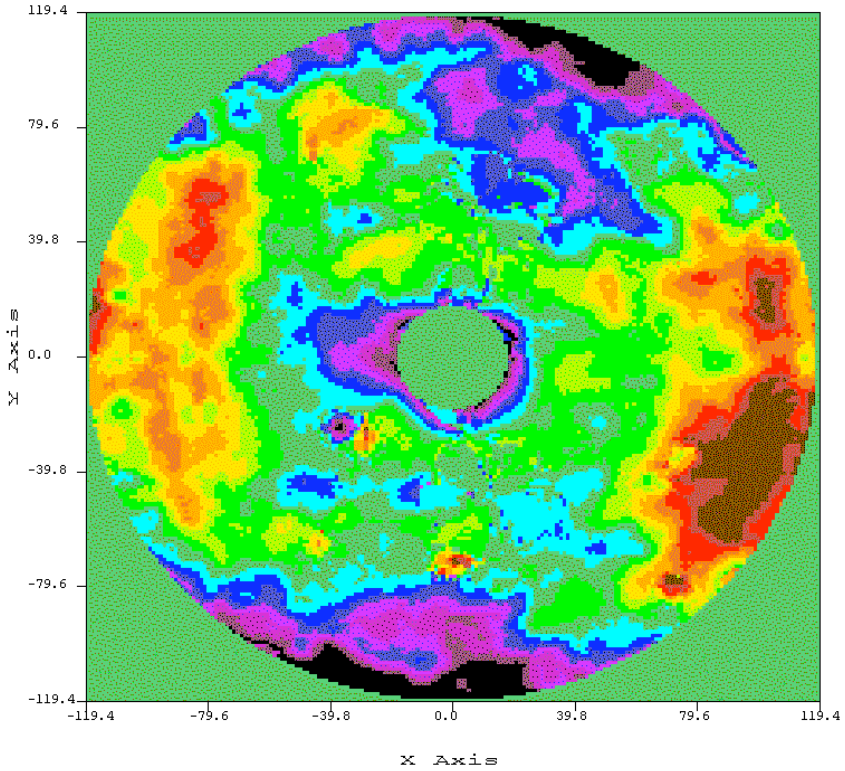

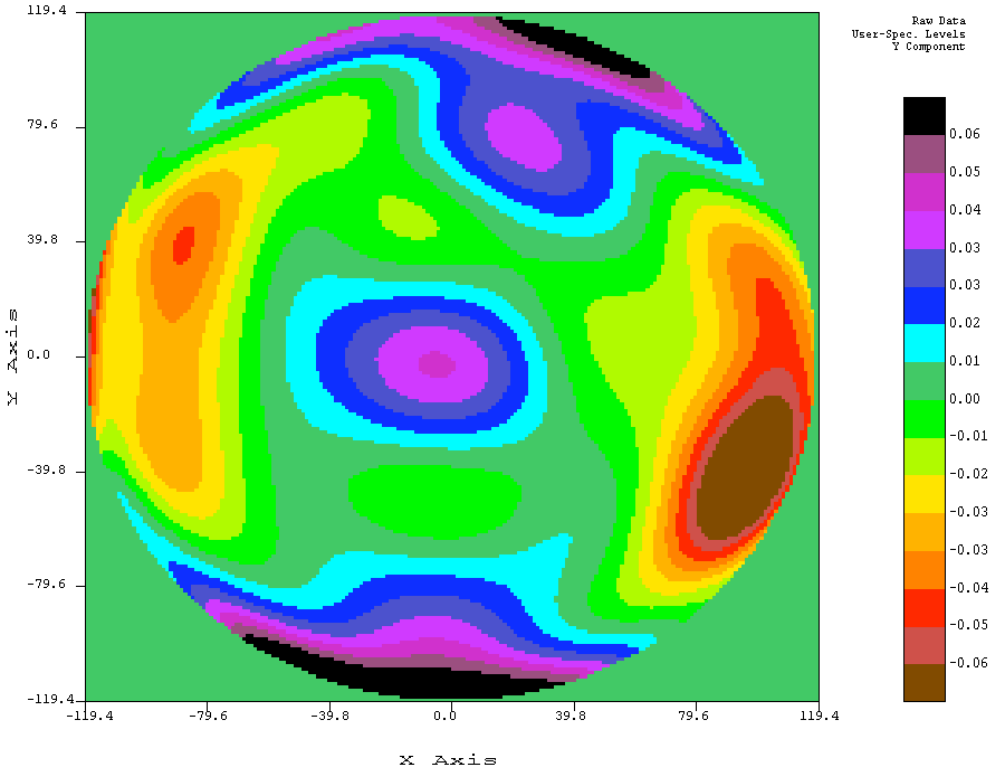

Distortion Recovery Algorithm using an array feed in focal region

- Statement of Problem:
  - Given the amplitude and phase received at each element of the array feed compute the main reflector distortion
- Solution:
  - From the signals received at the array feed estimate the Focal Plane Fields
  - Using the Focal Plane Fields compute the reflector distortion

Estimate the Focal Plane Fields

- Postulate a Fourier Series representation of the Focal Plane Field with unknown coefficients c_{nm}
- Convolve the Focal plane fields with the feed aperture distribution to write an expression for the feed response in terms of the unknown coefficients
- Using the measured feed response, solve for the coefficients using least squares as a maximum likelihood indicator

Compute the Reflector Distortions

- Conjugate the Focal Plane fields and then propagate them to the main reflector in the undistorted system
- Estimate the surface distortion by differing the phase from these fields to the fields computed from an undistorted system (determines negative surface)
- Compensate for any intermediate distortion using ray tracing

Recovery of Zernike (2,2) distortion

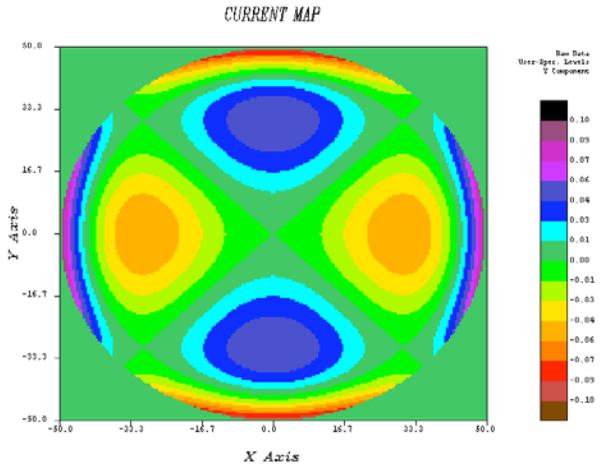

Distortion
Zernike (2,2)

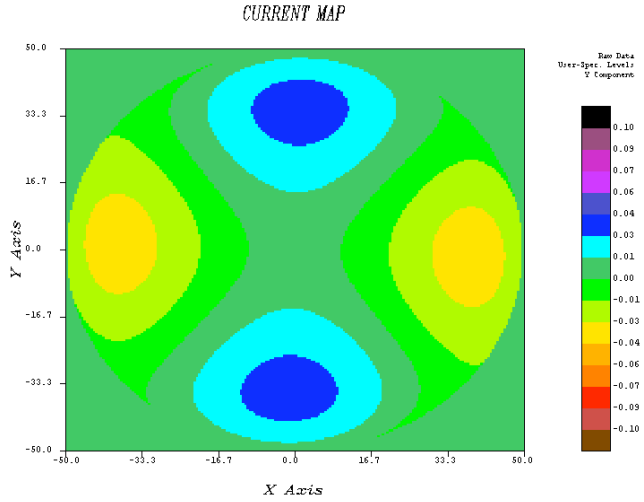

6 x 6 wavelength Focal Plane

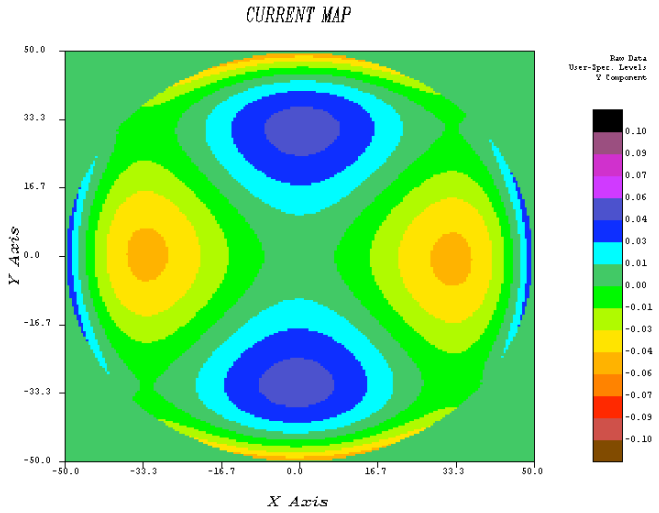

8 x 8 wavelength Focal Plane

Subreflector Probe Method

- The subreflector probe method is based on measuring the phase error at certain probe positions on the subreflector
- The probe positions are determined by applying the Circular Sampling Theorem on the main reflector and mapping those points to the subreflector via ray optics
- Application of the sampling theorem guarantees the minimum number of probes for a given order of distortion

Subreflector Probe Method

- The methodology will be based on a combination of geometrical optics (ray optics) and physical optics calculations.
- Using the circular sampling theorem if the values of the phase function are known at a particular set of points on the aperture, then the coefficients of a summation representing the phase function are readily calculated. The higher the number of sample points selected on the aperture, the larger the number of radial and azimuthal frequency components of the phase function that can be obtained.
- A set of points that satisfies the requirements for the circular sampling theorem are selected on the main reflector.
- The points are mapped via ray optics to points on the subreflector. The probes are placed at these points.
- Using a Physical Optics calculation the phase difference between an undistorted and distorted main reflector is determined at the subreflector probes.
- This phase difference is mapped back to the Main reflector and the distortion that produced the probe response is determined.

This technique was developed by Vahraz Jamnejad

Circular Sampling Theorem using Zernike functions

Any scalar function (or a scalar component of a vector function), $f(\rho, \phi)$ over a unit circle may be represented as a sum of Zernike or circular polynomials which are a complete set of orthogonal separable functions of the variables ρ and ϕ over the unit circle. The function must be truncated for numerical evaluation. The degree of truncation depends on the desired level of accuracy.

$$f(\rho,\phi) = \sum_m \sum_n B_m^n R_m^n(\rho) e^{jn\phi}$$

$$m = 0,1,2,...,\infty$$

$$n = \begin{Bmatrix} \pm 1, \pm 3, \pm 5, ..., \pm m, \ for\, odd\ m \\ 0, \pm 2, \pm 4, ..., \pm m, \ for\, even\, m \end{Bmatrix}$$

$$R_m^n(\rho) = \sum_{l=0}^{(\frac{m-n}{2})} \frac{(-1)^l (m-l)!}{l![(m+n)/2-l]![(m-n)/2-l]!} \rho^{m-2l}$$

Circular Sampling Theorem using Zernike functions-cont.

The coefficients B_{mn} *can be obtained approximately from a summation over a set of sample values and corresponding weights.*

The error in this approximation will be zero if the highest radial and azimuthal frequencies are less than or equal to $2m+1$ and $2n+1$, respectively. This would indeed be the case if the function $f(\rho,\phi)$ is exactly represented by the terms of radial and azimuthal frequencies less than or equal to m and n, respectively.

$$B_m^n = \sum_{i=1}^{m_u+1} \sum_{l=1}^{n_u+1} \frac{\pi w_i}{n_u+1} f(\rho_i,\phi_l) R_m^n(\rho_i) e^{-jn\phi_l}, \quad m \le m_u,\ n \le n_u$$

$$\phi_l = \frac{2\pi l}{n_u+1},\ \rho_i :\ zeros\ of\ \ h_{m_u+1}(\rho_i) = 0$$

$$h_m(x) = \sum_{l=0}^{\left\lfloor \frac{m}{2} \right\rfloor} \frac{(-1)^l (m-l)!}{l!\left(\left\lfloor \frac{m+1}{2} \right\rfloor - l\right)!\left(\left\lfloor \frac{m}{2} \right\rfloor - l\right)!} x^{m-2l},\ m = 0,1,\ldots,\infty$$

Circular Sampling Theorem- Cont.

Some typical sampling point distribution and corresponding weight functions

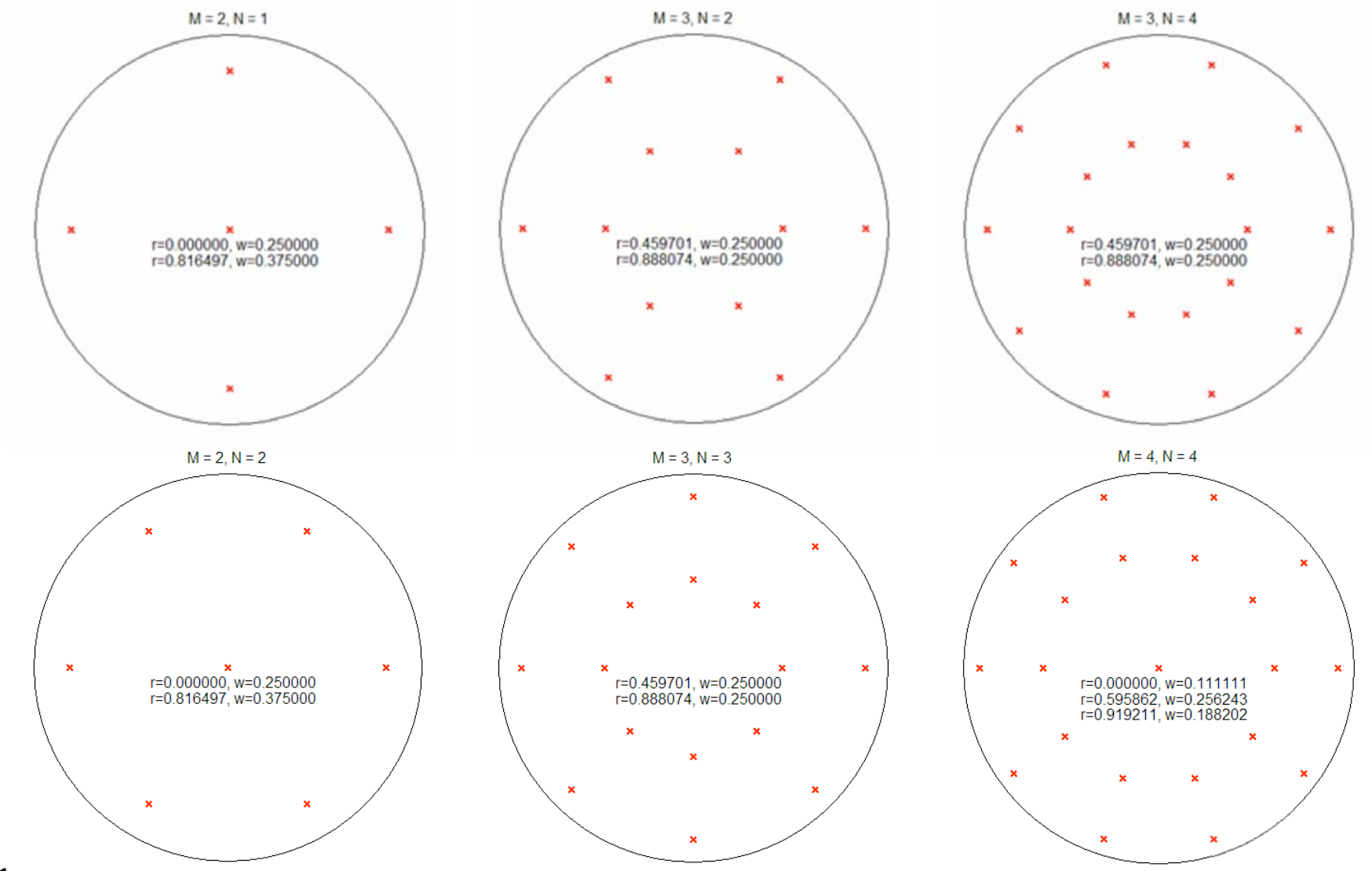

Methodology

- The reflector surface error is represented by a Δz error function as a sum of Zernike polynomial functions on the circular aperture of the reflector.
- Ray optics is used to map the points on the main reflector to the subreflector
- The phase error (corresponds to surface error) is measured at the probe points on the subreflector
- The errors on the subreflector are mapped onto the main reflector
- The sampling theorem is used to obtain the complete reflector profile

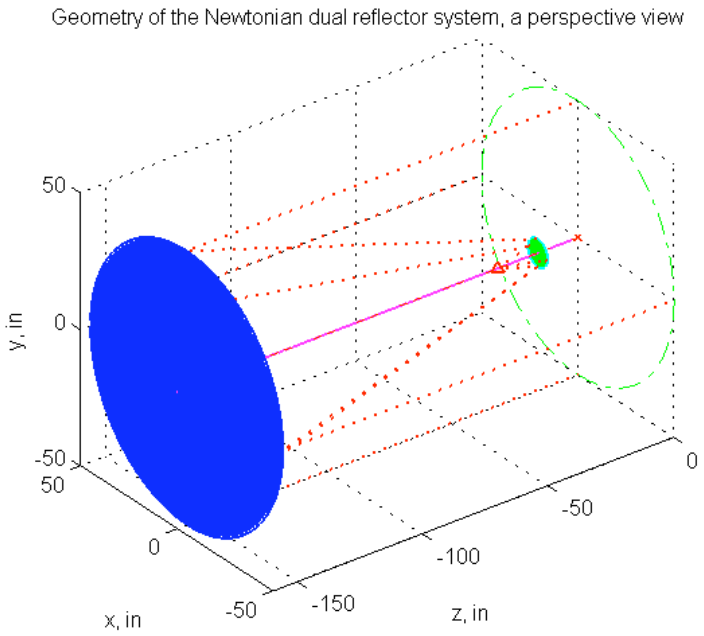

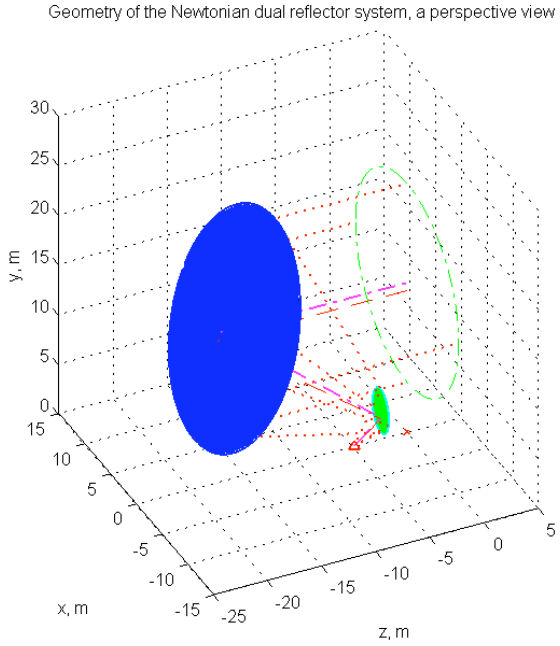

Example geometry

- The main or primary reflector is an offset parabolic reflector, while the sub or secondary reflector is a flat reflector.

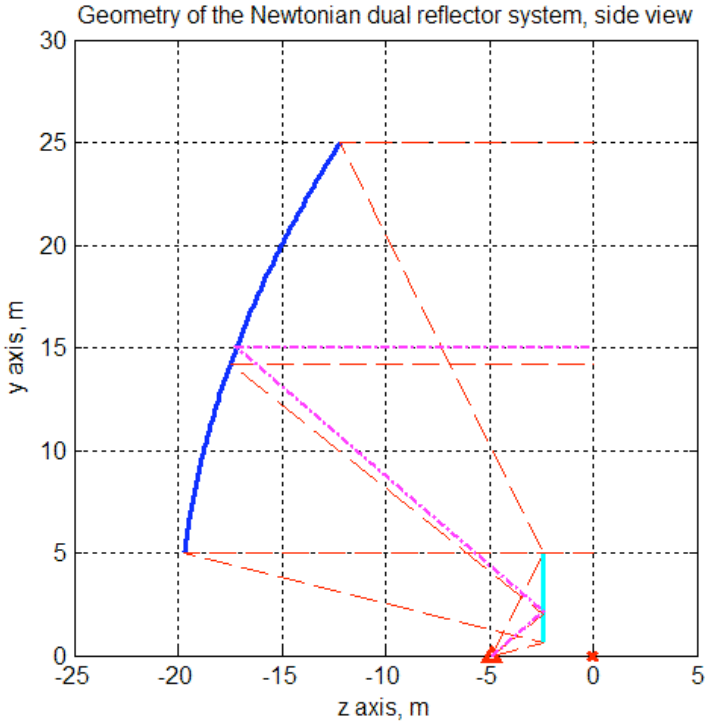

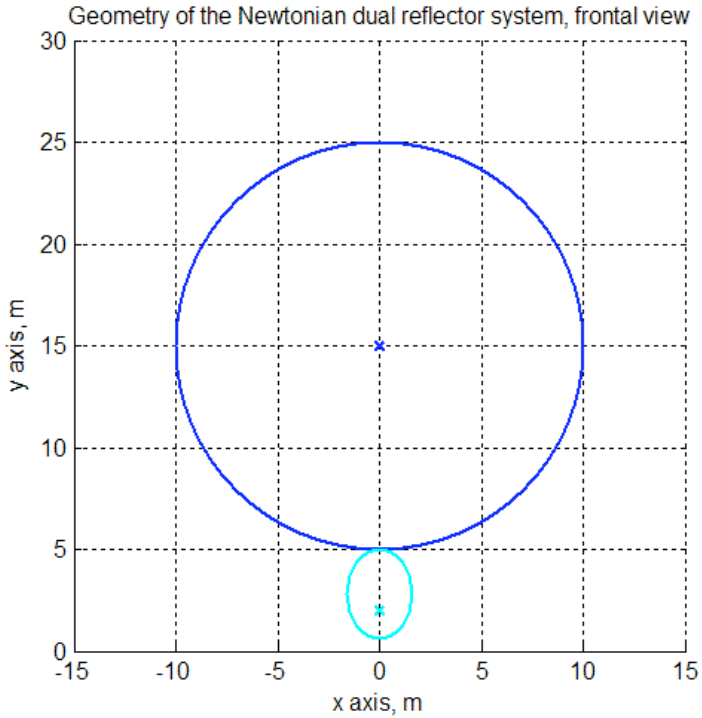

Selection of Sample Points

- A set of sampling points are selected on the main reflector aperture and their corresponding points on the sub-reflector are determined via ray optics.
- The sample points are selected base on a Zernike functions-bases circular sampling theorem. The 21 sample points shown are sufficient to represent radial and azimuthal terms of up to degree 4.

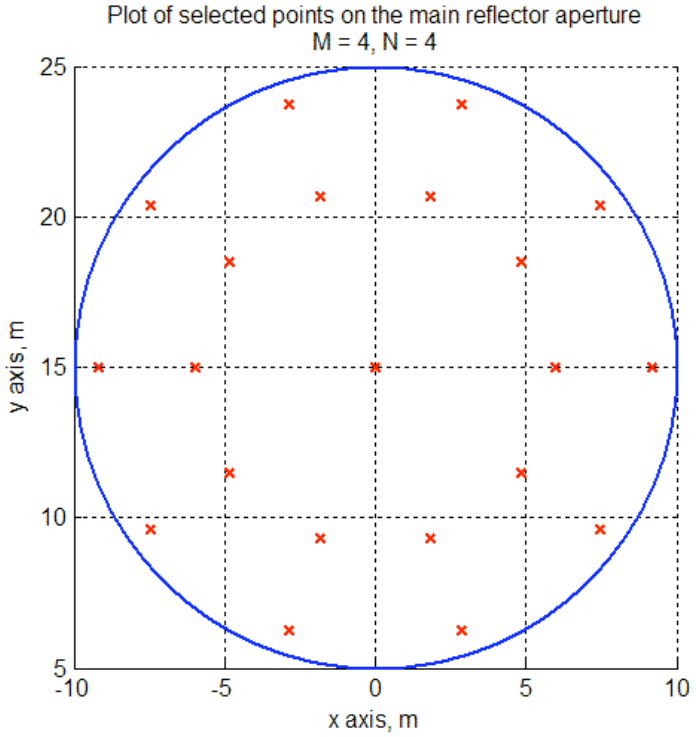

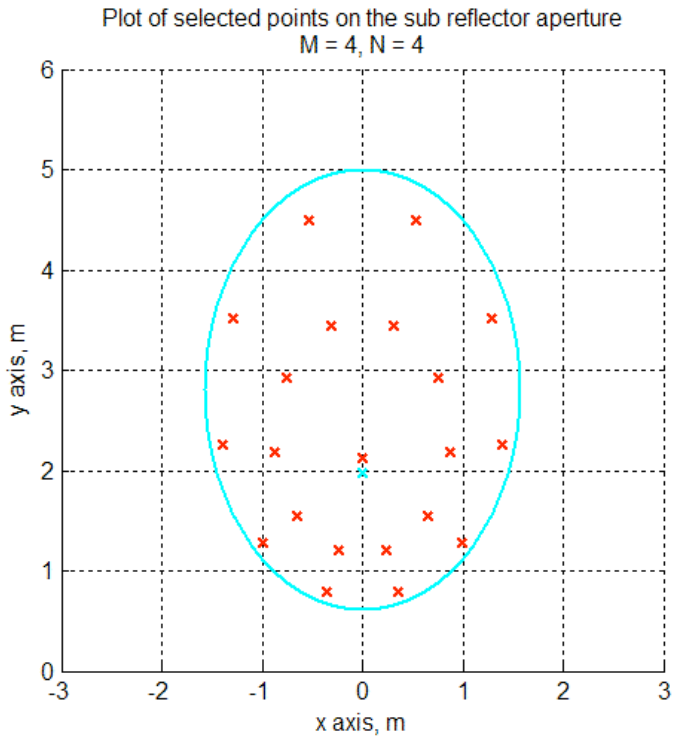

Sample error function

- The reflector surface error is represented by a Δz error function as a sum of Zernike polynomial functions on the circular aperture of the reflector.

- A typical Zernike function of radial order 3 and azimuthal (angular) order 3 is shown below. Such a surface error, or a combination of such functions up to order 4 in both azimuth and radial directions can be completely recovered by the sample points on shown on the previous page.

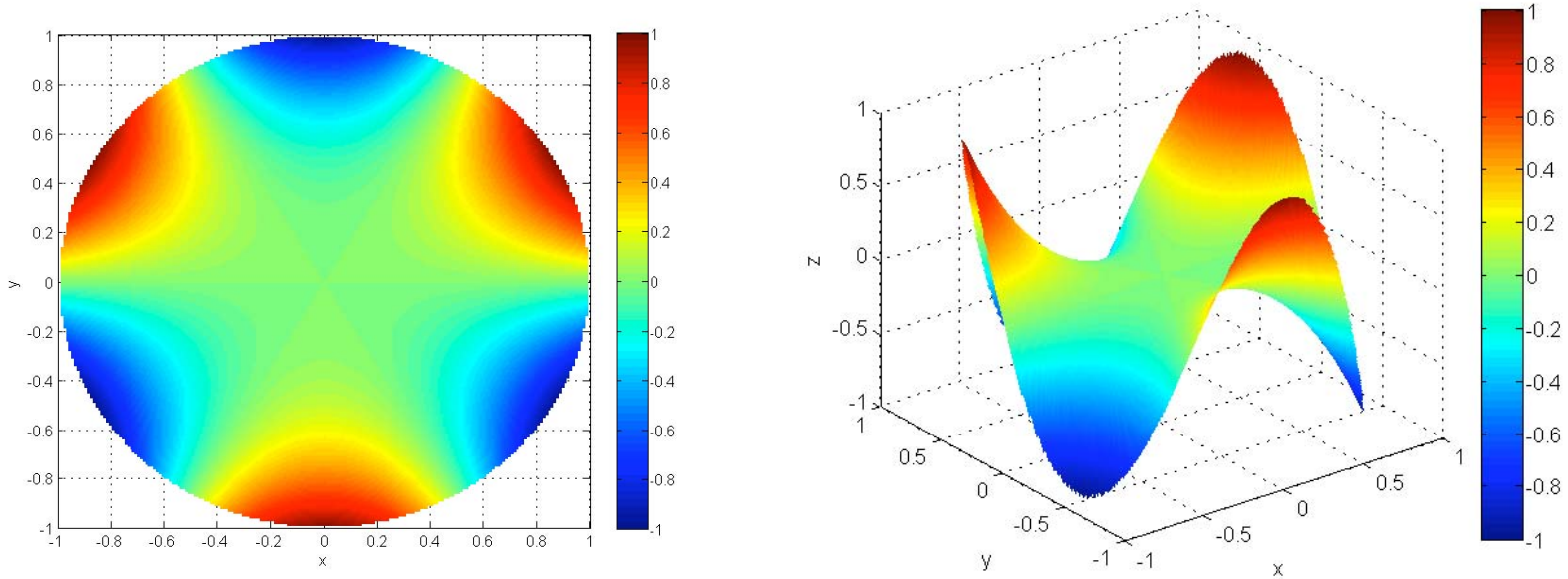

color contour plots of the function $\rho^3 \sin(3\phi)$ (Zernike serial order 10)

Example: 3rd order distortion

- As an example of a possible phase distortion the following function is considered.

$$\Delta z = \varepsilon \rho^3 \sin(3\phi)$$

- In this function ε is selected such that it could result in 3 db loss:

$$\varepsilon / \lambda = 0.1871, \ \varepsilon = 0.00561 \text{ m} = 5.61 \text{ mm}$$

- The sampling method is applied with M=4, N=4. By using sample values at locations given in Figure on the next page and the Table below, with appropriate weights, the original function is exactly recovered. It should be emphasized that this sampling arrangement will recover any functions of orders up to 4 in both radial and azimuthal directions and any combination of such functions.

Sample values versus positions and weights *with sampling orders M=4, N=4.*

Weight	$\rho \downarrow \quad \phi \rightarrow$	36°	72°	*108°*	144°	180°
0.188202	*0.919211*	0.240009	0.628352	-0.6284	-0.240009	0.776684
0.256243	*0.595862*	0.065376	0.171157	-0.171157	-0.065376	0.211561
0.111111	0.000000	0	0	0	0	0
0.256243	*0.595862*	-0.065376	-0.171157	0.171157	0.065376	-0.211561
0.188202	*0.919211*	-0.240009	-0.628352	0.628352	0.240009	-0.776684

Physical Optics analysis and verification

- The selected case is analyzed using a physical optics analysis program.
  - 1- First the error free reflector is considered. Currents on the surface of the sub reflector due to an incident uniform plane wave on the main reflector aperture are computed.
  - 2- The phases of the currents at the selected sampling points are calculated.
  - 3- Then an error is introduced on the reflector surface, and the currents are recalculated.
  - 4- The difference between the two set of values calculated in the previous two steps are obtained.
  - 5- These error samples are then transferred to the sample points on the circular aperture of the reflector via ray optics.
  - 6- Using the sampling theorem discussed before the error function is recovered.
  - 7- This function is then compared to the original error function introduced on the reflector, for validation and accuracy.
- The results are graphically presented on the following pages.

Calculation of phase at sample points on sub-reflector by Physical Optics and Ray Optics

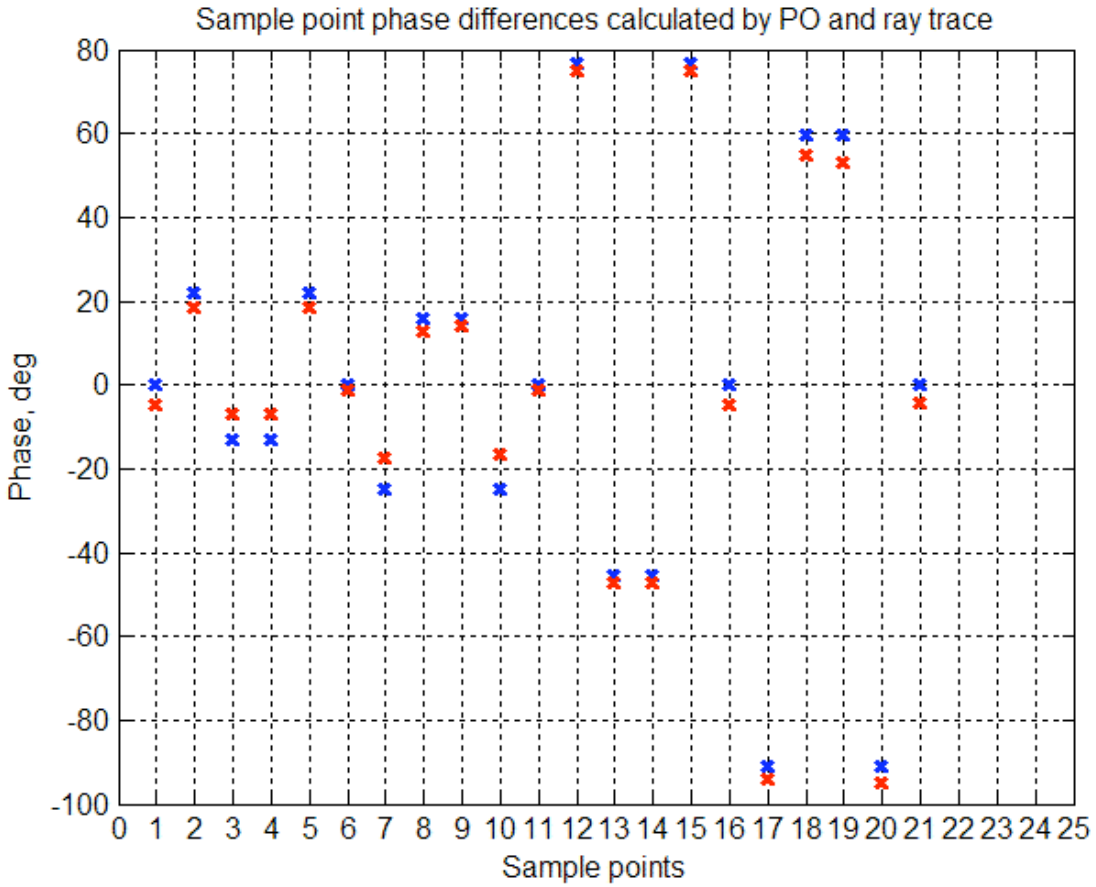

Original and reconstructed phase contours

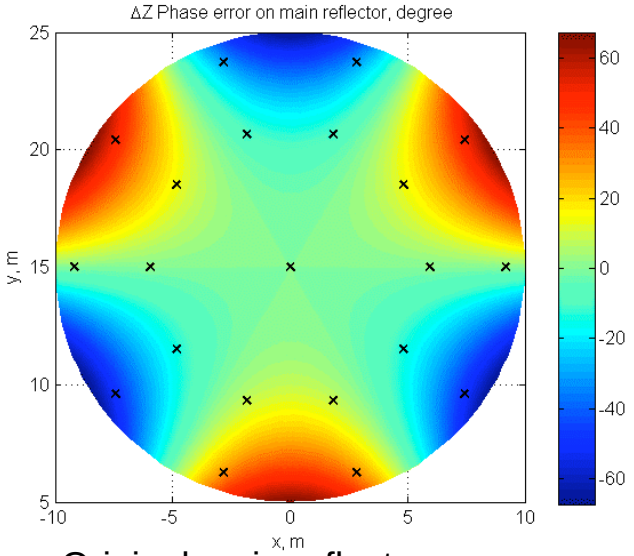

Original main reflector error

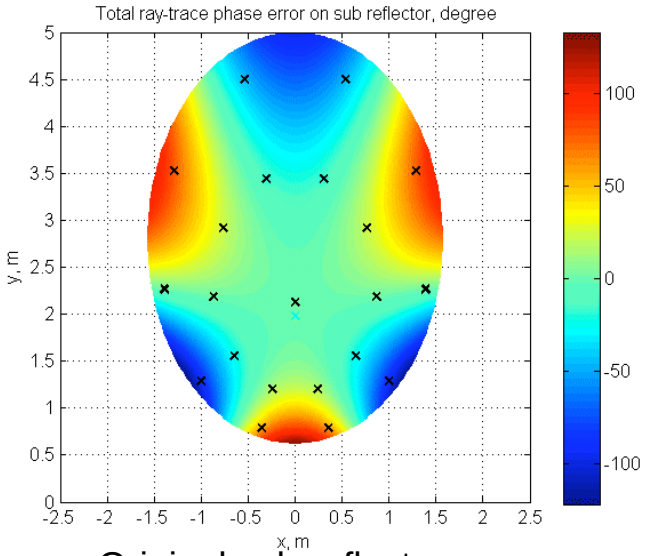

Original sub-reflector error

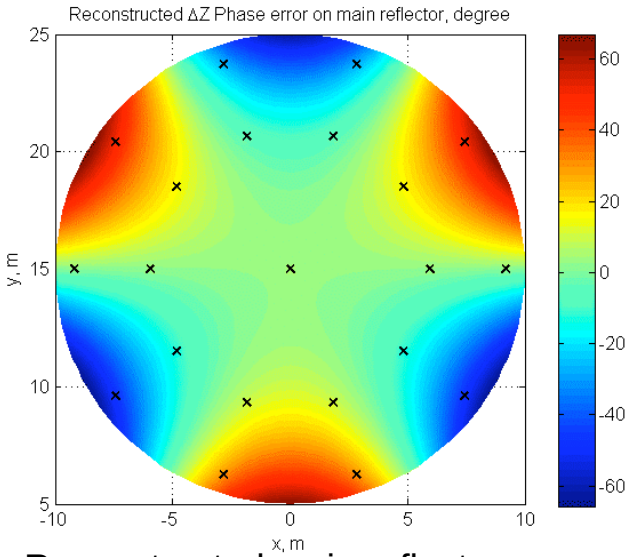

Reconstructed main reflector error

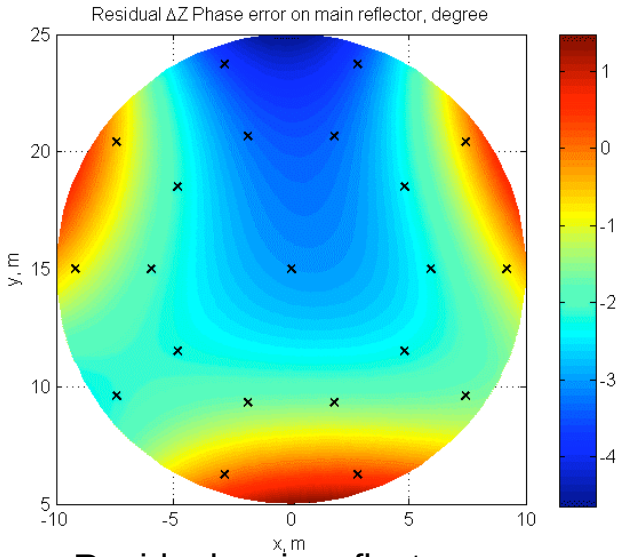

Residual main reflector error

Proposed Experiment

- It has been demonstrated that by sampling the phase on the planar sub-reflector on a limited set of points (21 in this case) and using Physical Optics, the reflector distortion can be calculated with a high degree of accuracy and minimal residual error. This set of points are sufficient for all errors of the radial and azimuthal order 4.
- The actual sampling must be performed using feed probes (microstrip patches, e.g.). The next step is an actual hardware demonstration of the technique using a 48 inch reflector at 32 GHz.

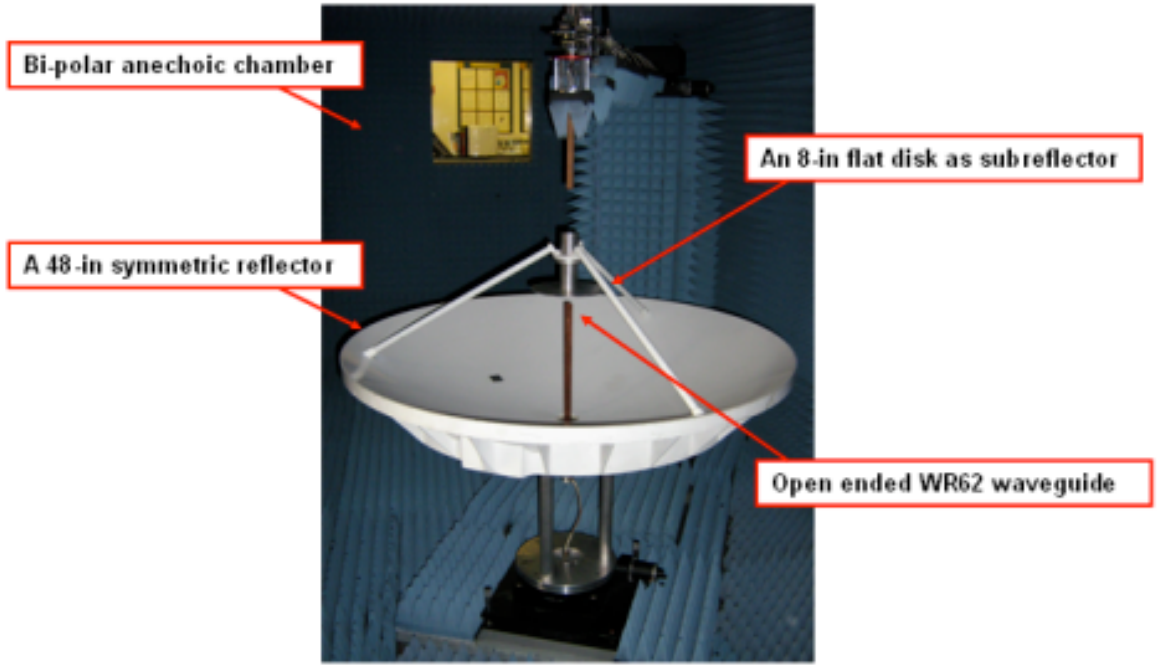

A sketch drawing of patch antenna with 0.254 mm (10 mil) thick Foam substrate

Center frequency: 32 GHz (Wavelength= 9.369 mm = 0.3688”)
(not to scale)

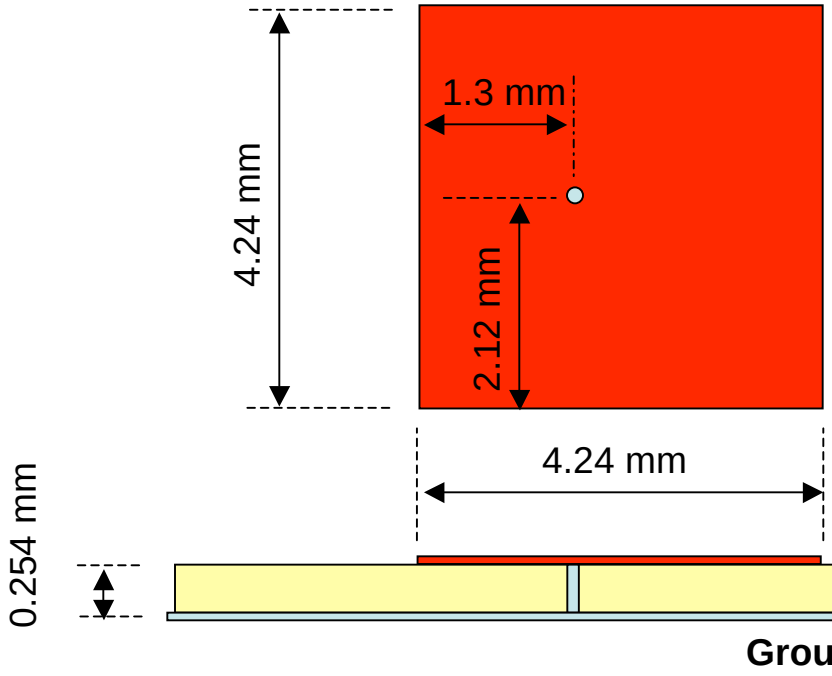

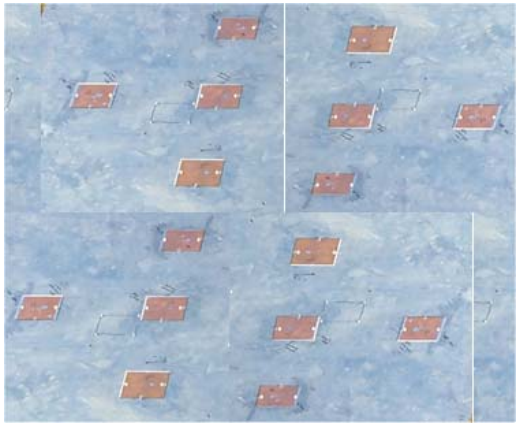

Sample Patches

Phase correcting reflectarray

Undistorted main

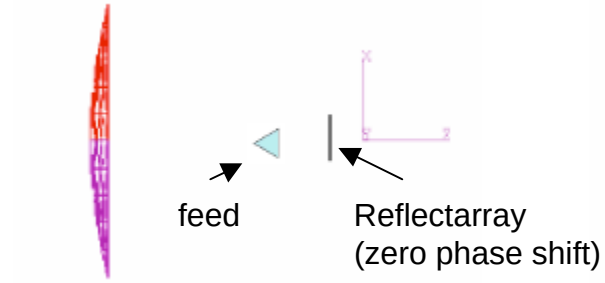

Distorted main

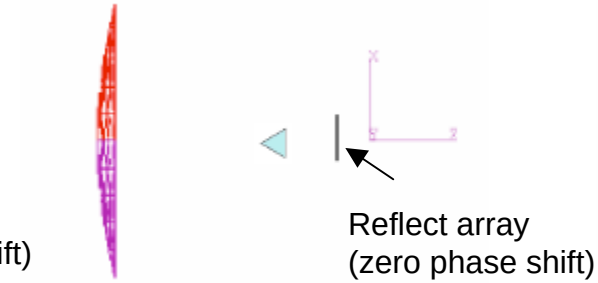

Distorted main

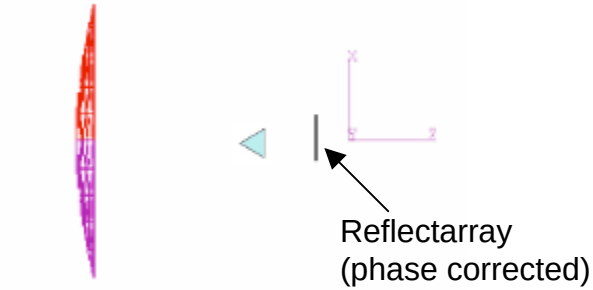

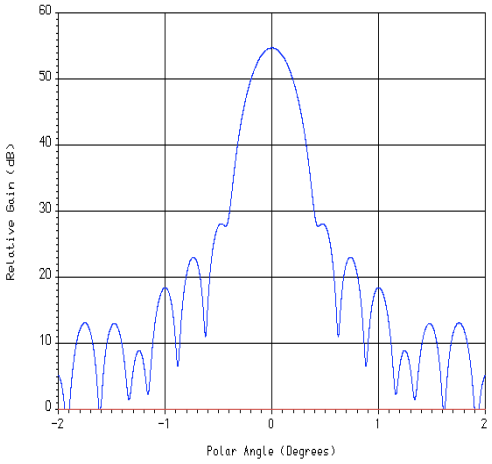

Gain = 54.73 dB

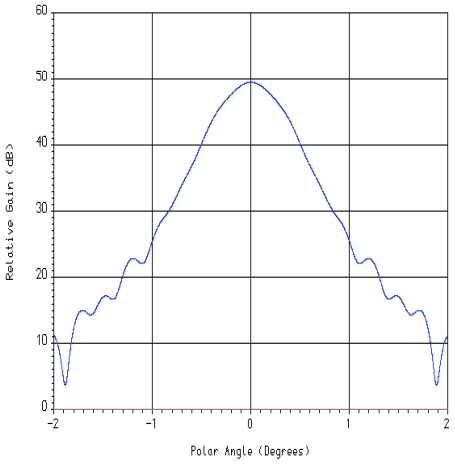

Gain = 49.54 dB

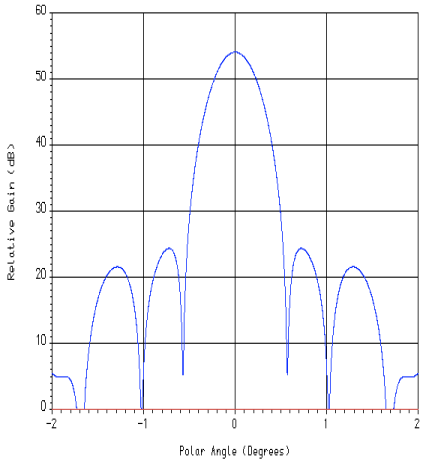

Gain = 54.09 dB

Phase correcting reflectarray

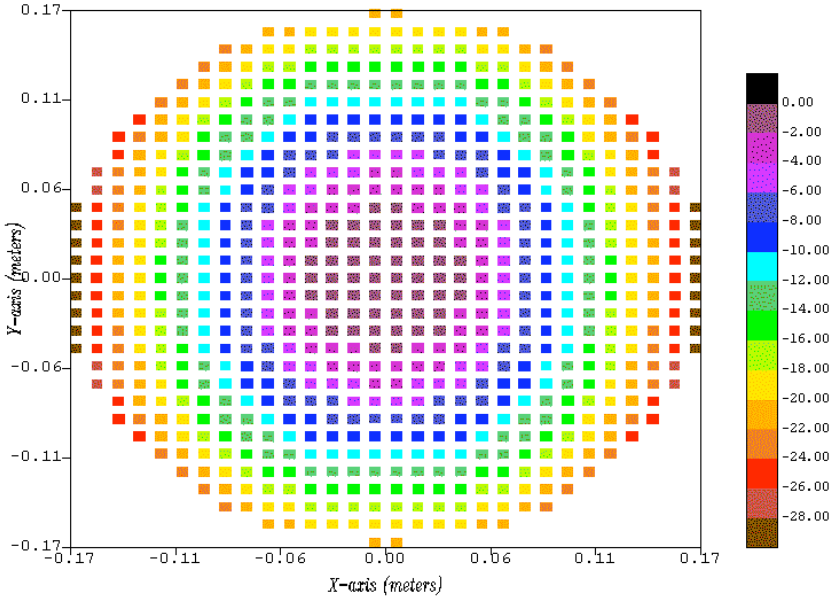

Patch Array
Phase shift by unequal patch size

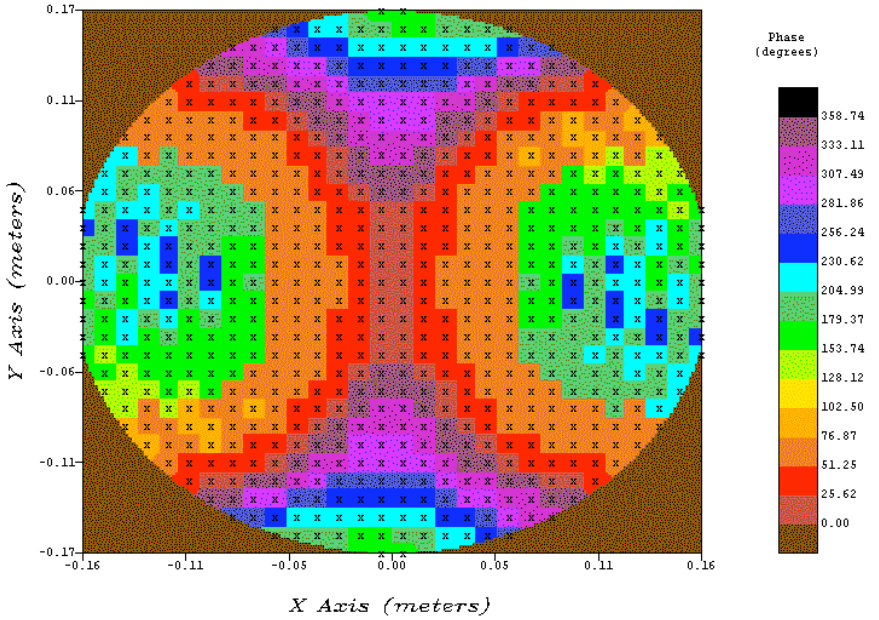

Required phase shift computed by conjugate phase method

Geometry – D = 5 meters, F/D = 1.0 distortion $\Delta z = \varepsilon\rho^2\cos(2\varphi)$
Frequency = 13.285 GHz ε = 7.5 mm Feed – n=11.82

Experimental validation of reflectarray compensation technique

- The plan is to use a 48 inch reflector with an 8 inch flat reflectarray to compensate for a fixed distortion
  - Add representative distortion
- The phase adjustment will be accomplished with variable size patches
  - Design and fabricate compensating patch array
- Measurements will be made
  - With and without distortion with a flat disk as subreflector
  - With distortion and a phase compensating patch array

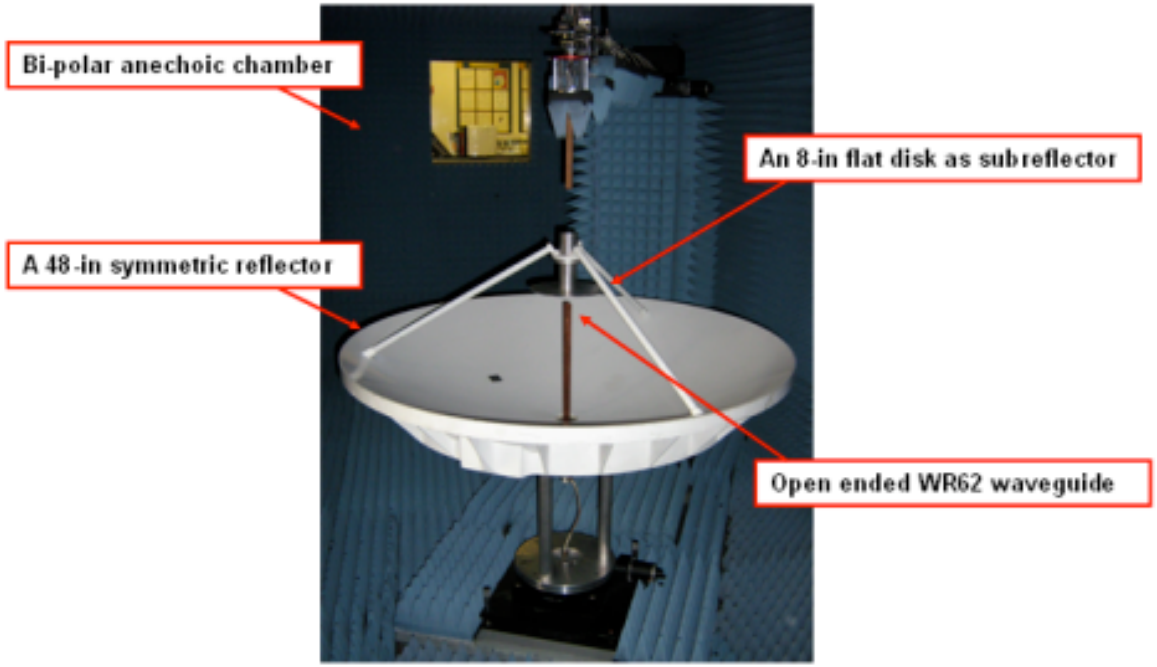

Potential Candidates for Reflectarray Element

Approach	PATCH	SLOT	STRIPLINE
Element (unit cell)	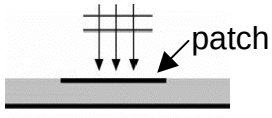	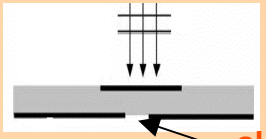	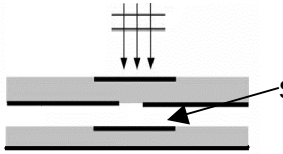
Reflection phase change mechanism	By varying the size of the patch	By varying the length of the slot	By varying the length of the stripline
Reconfigurable element using MEMS	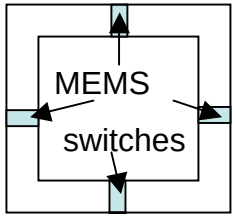	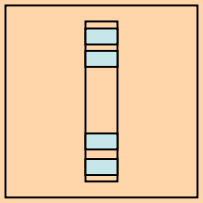	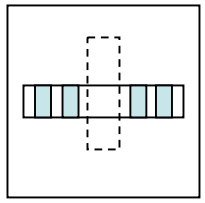
MEMS location and integration issues	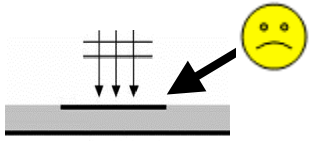 MEMS on top layer is not ideal	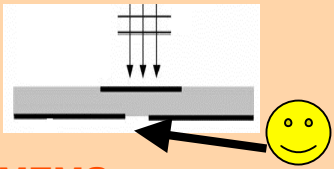 MEMS on ground plane	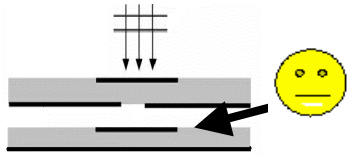 MEMS on a different layer

Variable Slot on Ground Plane

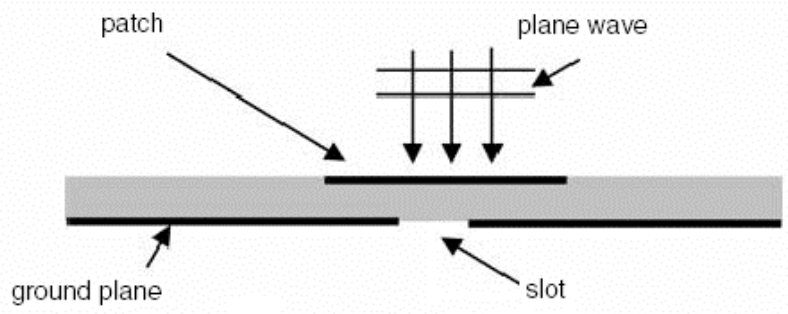

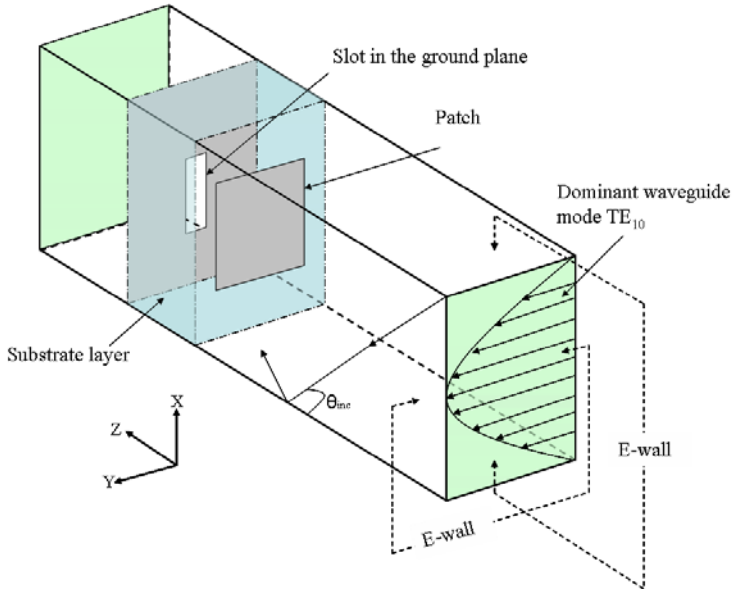

Waveguide simulation approach

- Radiating patch elements of identical size on the top layer and slots of variable length in the ground plane.
- Dimensions are chosen such that the slot acts as a load on the patch and the patch is close to resonance.
- The presence of slots acts as an inductive loading on the patches introducing a phase shift.
- As the slot length changes, the load on the patch changes and thus the reflection phase changes (due to shift in resonant frequency).

Characterization of reflectarray element – 60 mil

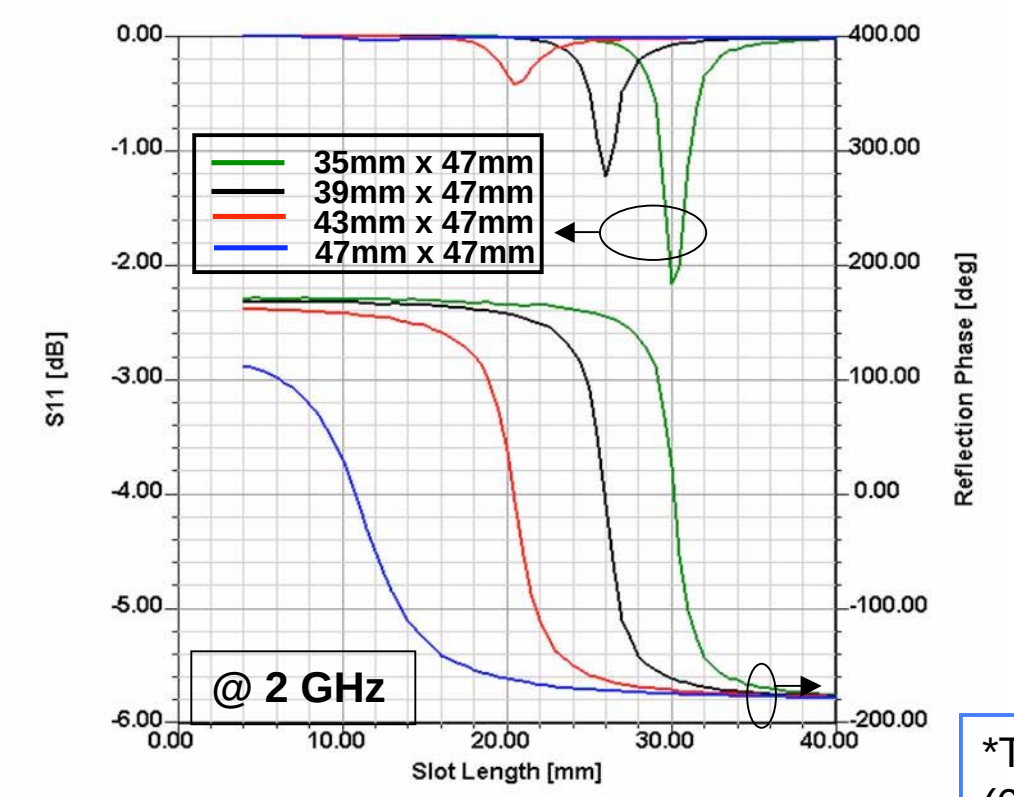

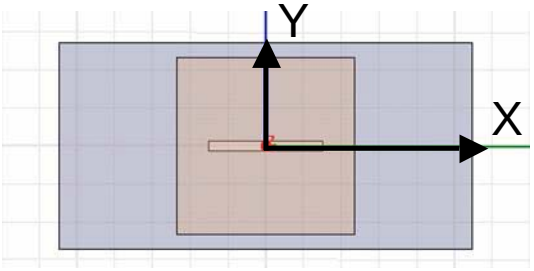

X-dimension of patch is constant
Y-dimension of patch is varied

X-dimension of slot is varied
Y-dimension of slot is constant

*As the patch dimensions increase, the loss decreases and slope of reflection phase also decreases.

*The simulation of the patch-slot element (60 mil) is performed. Here, dielectric loss tangent of substrate is assumed to be zero and both the patch and ground plane are assumed to be PEC.

Selection of patch and slot dimensions

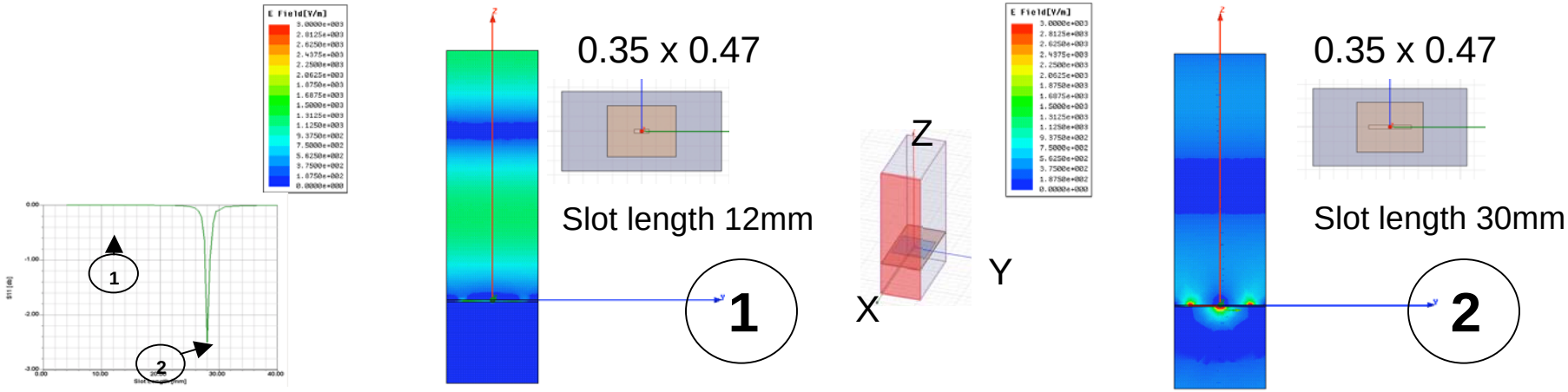

*When the patch dimensions are small, the loss is due to slot radiation. Dimensions are chosen such that the slot acts as a load on the patch and the patch is close to resonance.

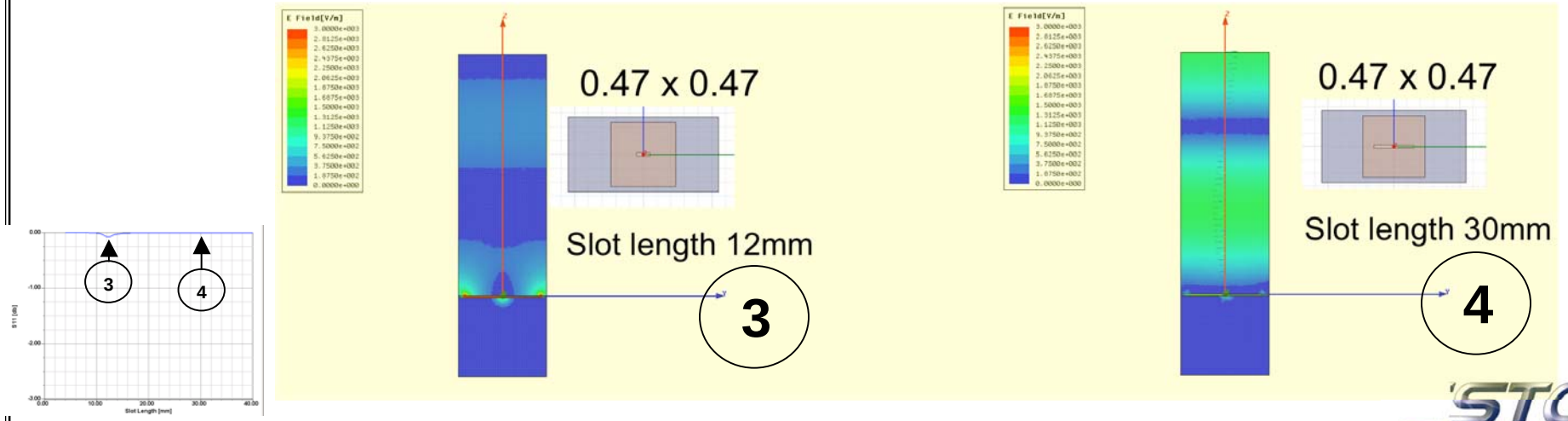

Reflectarray element – 60 mil

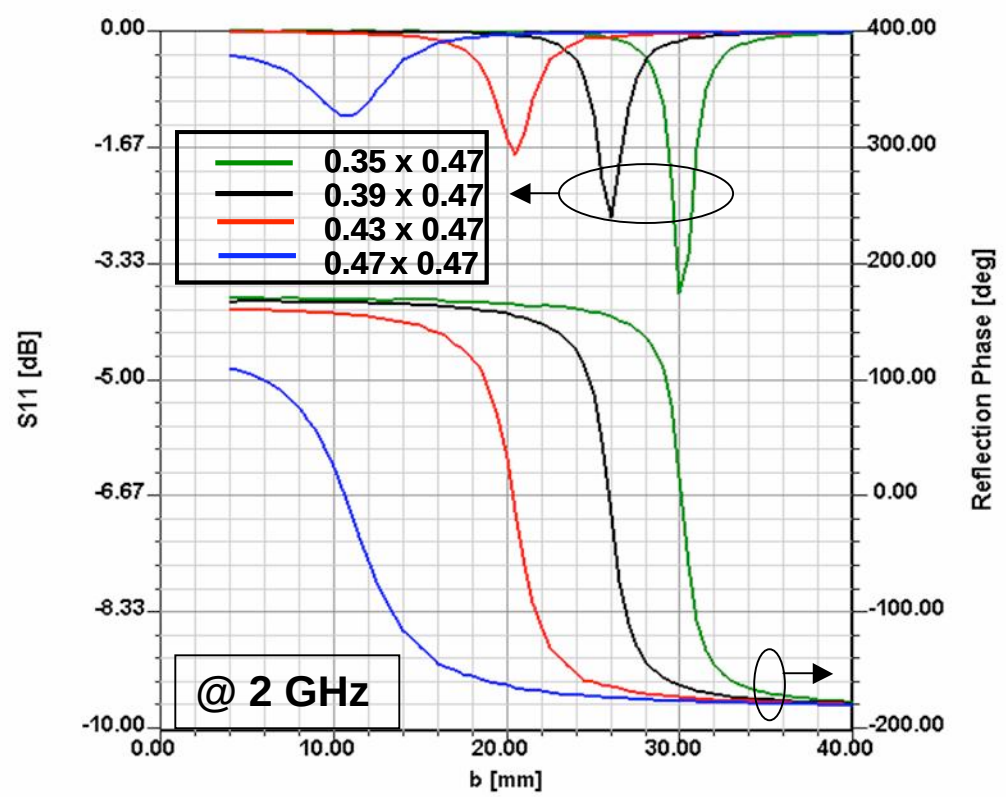

Substrate thickness - 60 mil

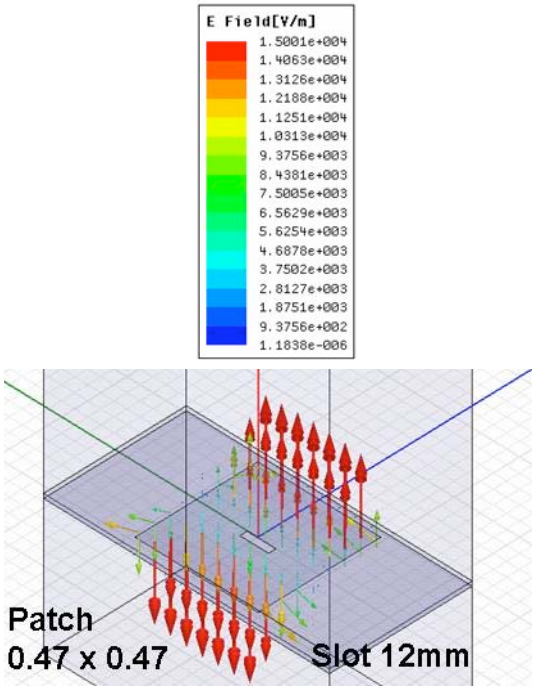

*Dimensions are chosen such that the slot acts as a load on the patch and the patch is close to resonance. The loss is minimum and the S-curve is smooth but the phase swing range decreases.

*The simulation of the patch-slot element (60 mil) is performed. Here, both dielectric and conductor loss are considered (affects S11 magnitude only).

RADANT MEMS – Driver board, Evaluation board and RF MEMS Switch

- **RADANT MEMS**
- SPST RF-MEMS SWITCH - DC to 12 GHz
- High Isolation (25 dB @ 2 GHz)
- Low Insertion Loss (0.15 dB @ 2 GHz)
- High Return Loss (-23 dB @ 2 GHz)
- Dimensions: 1.45mm x 1.45mm
- Actuation voltage: 90 V

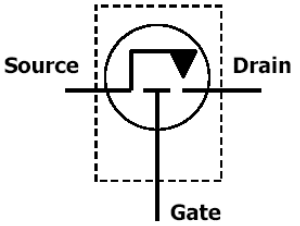

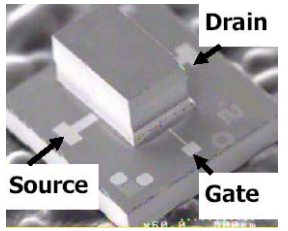

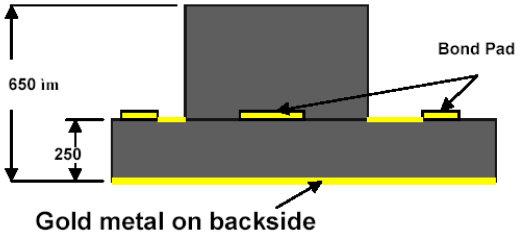

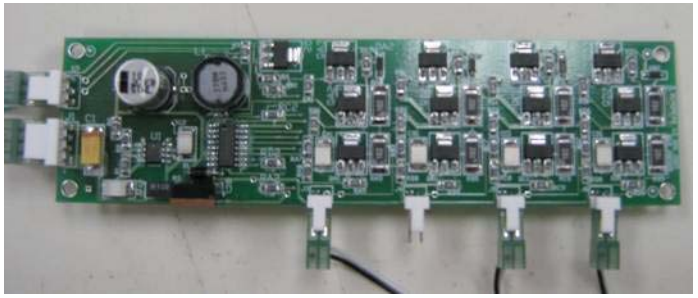

Driver Board

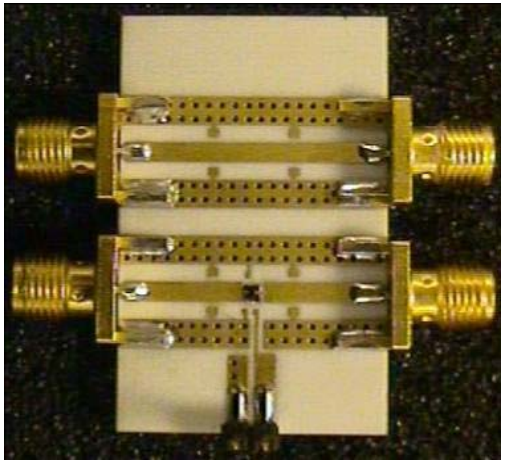

Evaluation Board

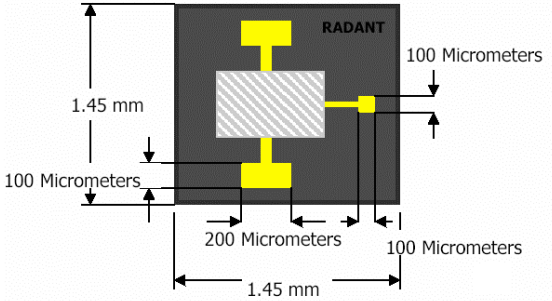

Microscopic view of the MEMS switches

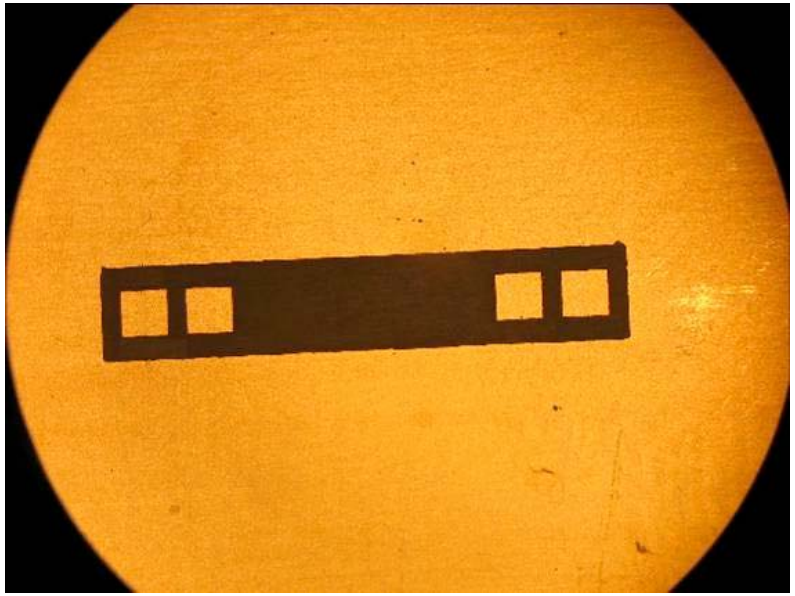

Sample with copper pads to mount the switches

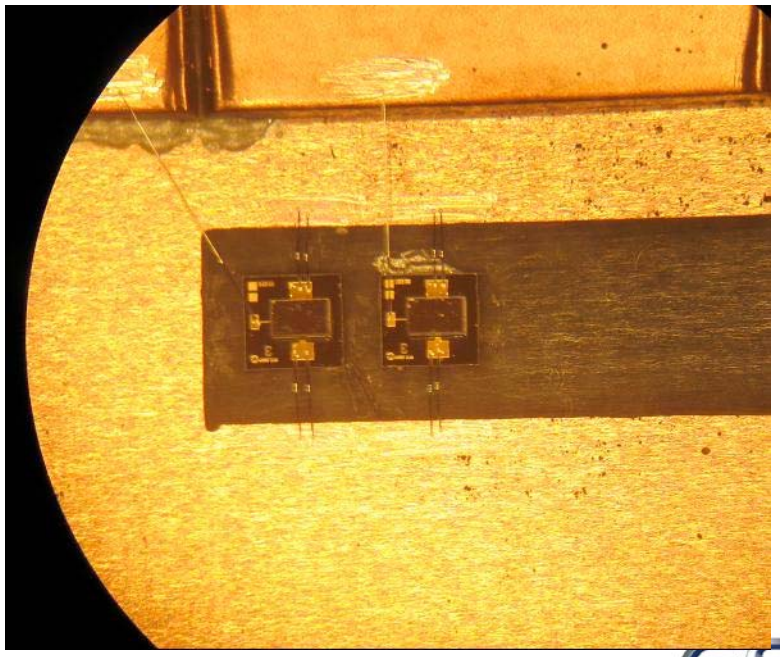

Experimental setup and 4 RF MEMS switches on the slot

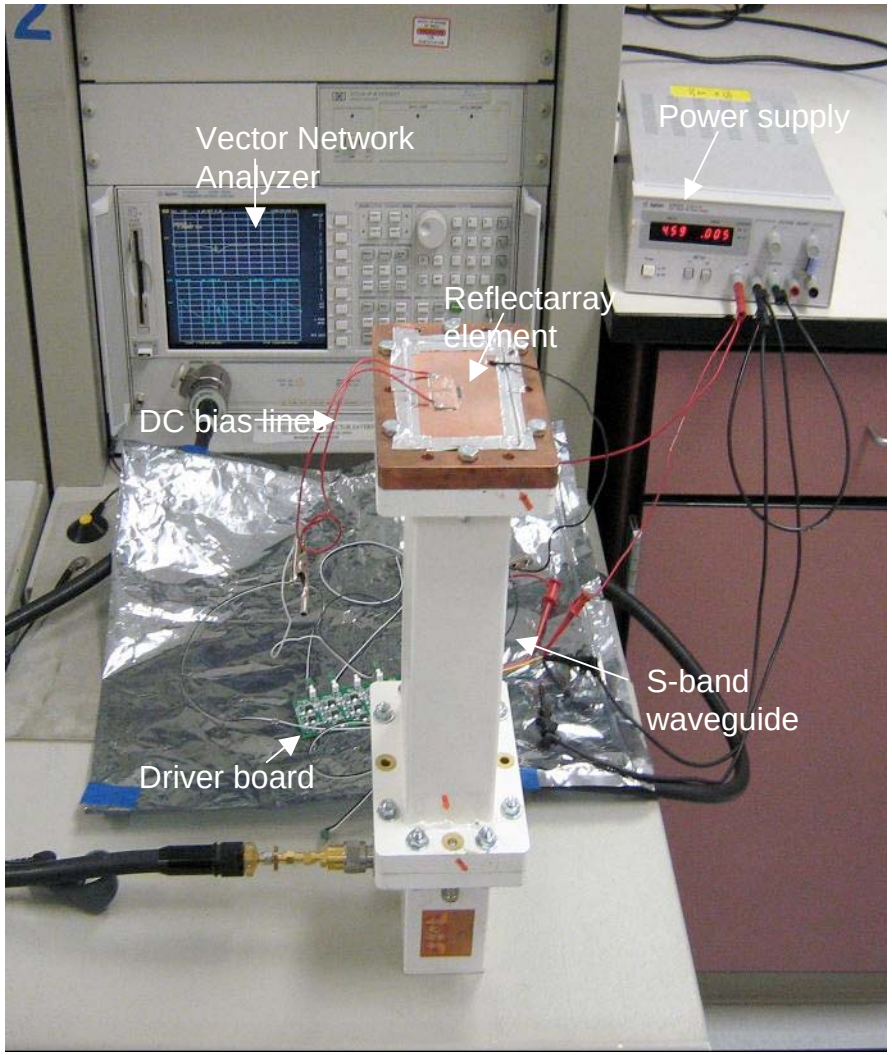

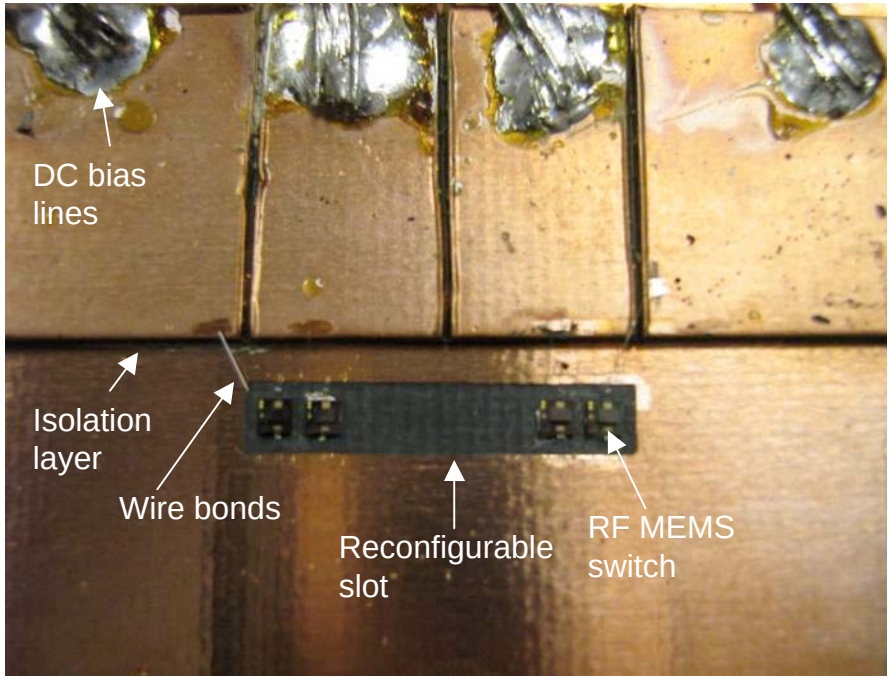

Screenshot from Network Analyzer

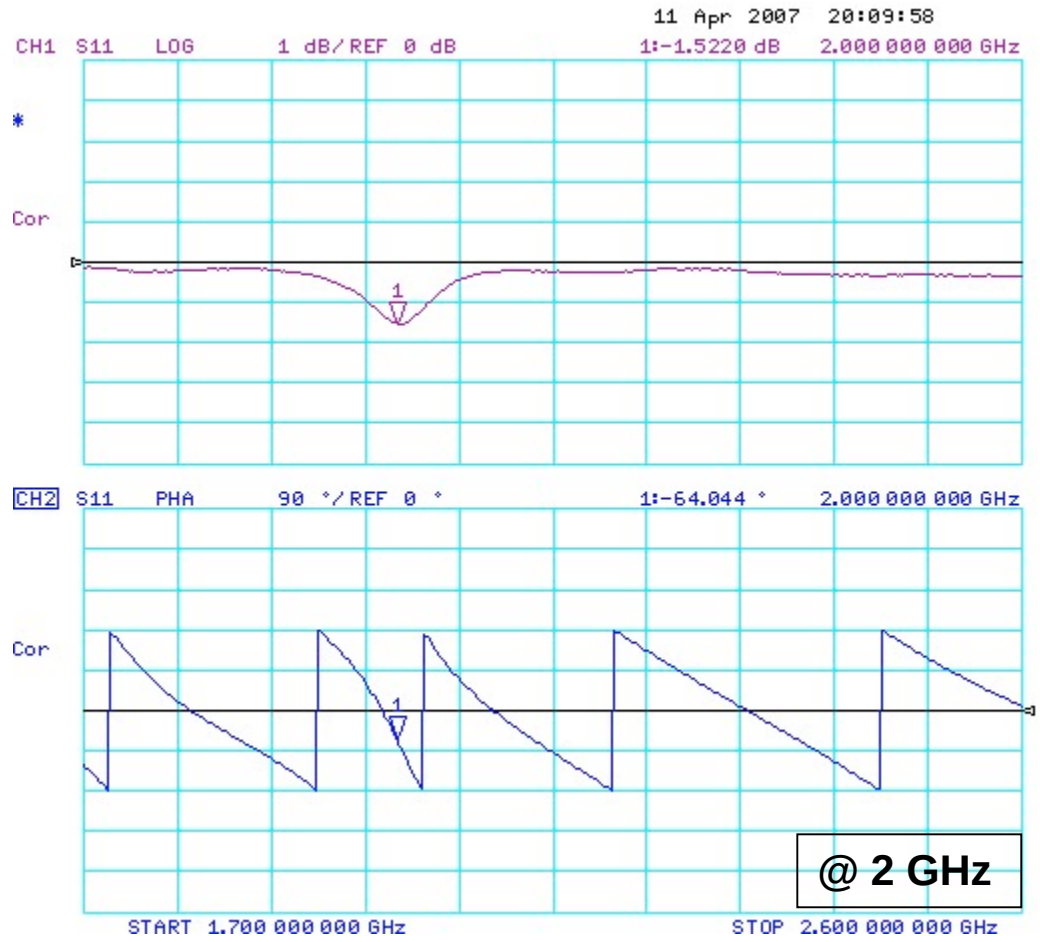

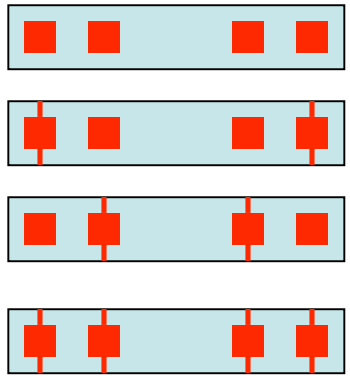

@ 2 GHz

**As the switches are turned on the effective slot length decreases which in turn increases the resonant frequency of the patch.

Measurement – S11 mag and phase

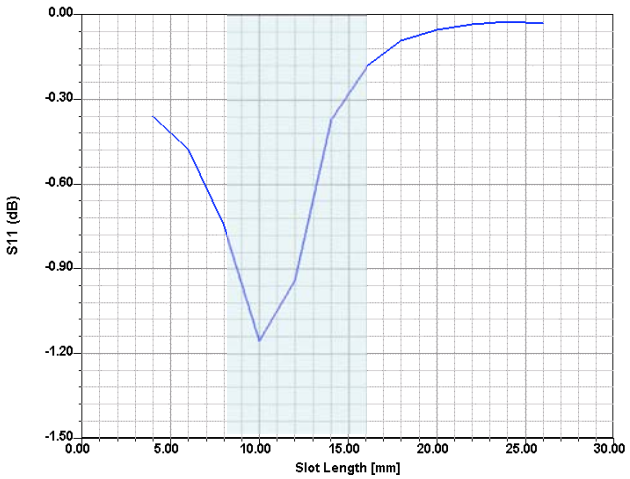

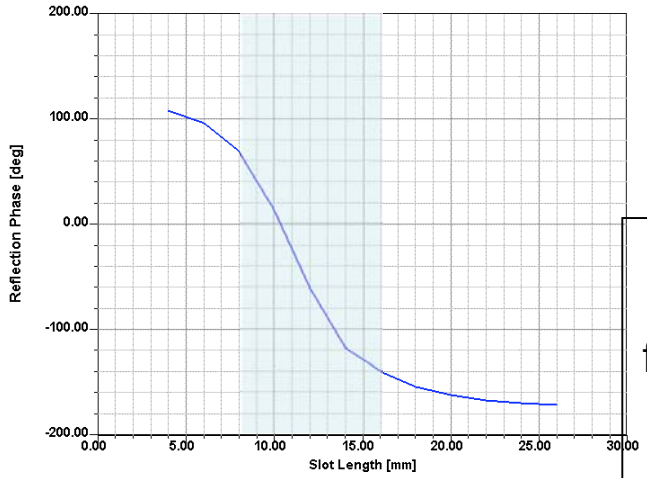

Switch State	Measurement S11(dB)	Measurement Phase (deg)
0	-0.47	-132.75
1,8	-0.64	-115.95
9	-0.89	-94.33
2,4	-0.93	-91.81
3,12	-1.05	-79.09
5,10	-1.31	-57.81
11,13	-1.41	-43.92
6	-1.57	-17.23
7,14	-1.58	1.04
15	-1.52	15.47

*The number of states (M) possible for N RF MEMS switches mounted over the entire slot is given by the formula described below (taking symmetry into consideration)

$$M = \{2^{N/2} + 1\} * \{2^{(N/2 - 1)}\}$$

Ideal switch, wire bond, MEMS switch - Comparison

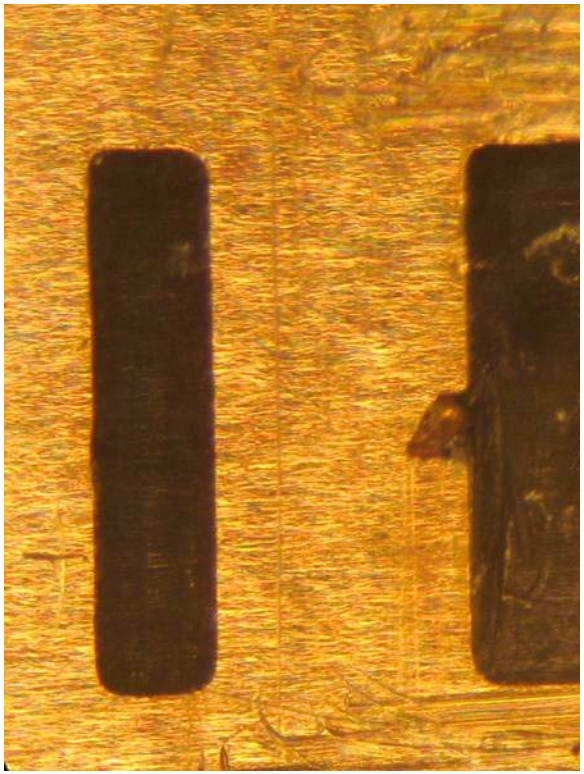

Ideal switch

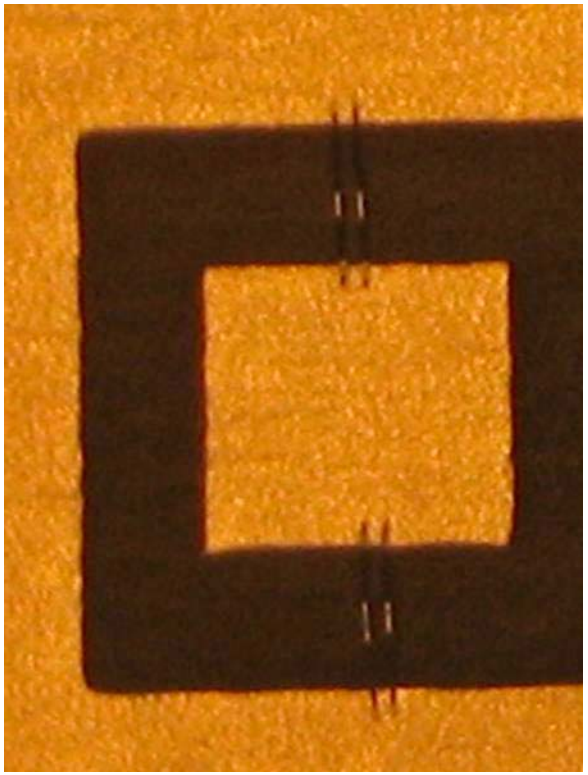

Wire bond

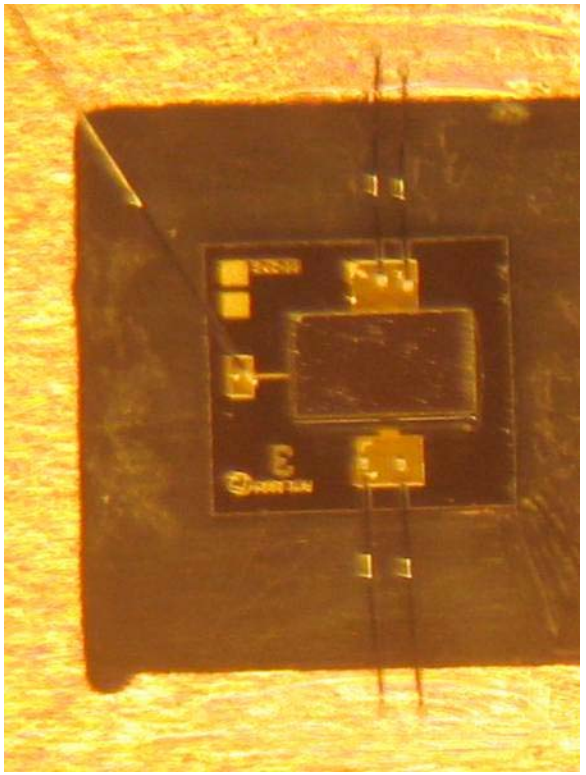

RF MEMS switch

Ideal switch (copper etched)

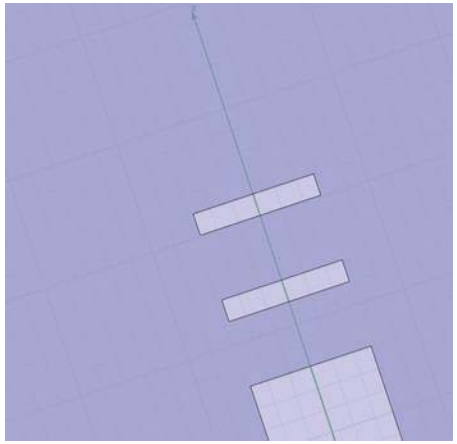

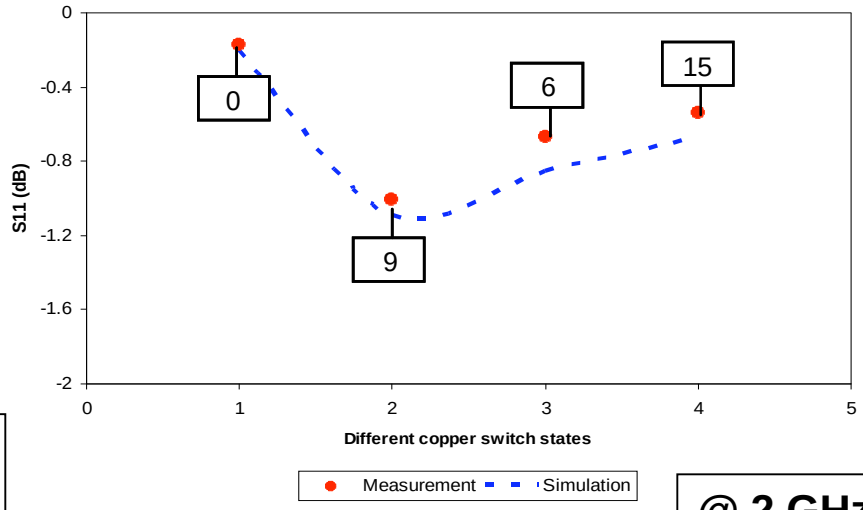

*The ideal switch shorts the slot width completely and the currents are concentrated at the edge of the active slot length.

@ 2 GHz

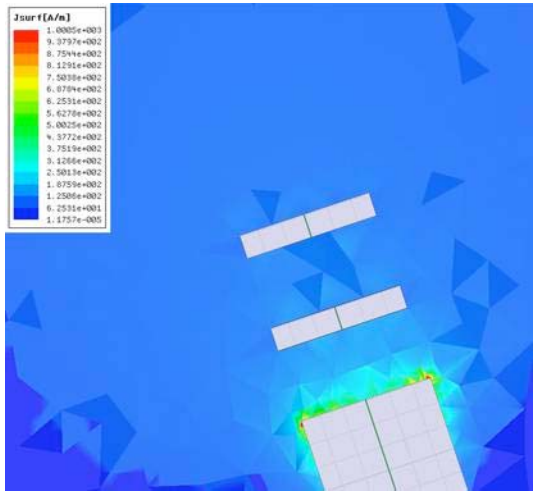

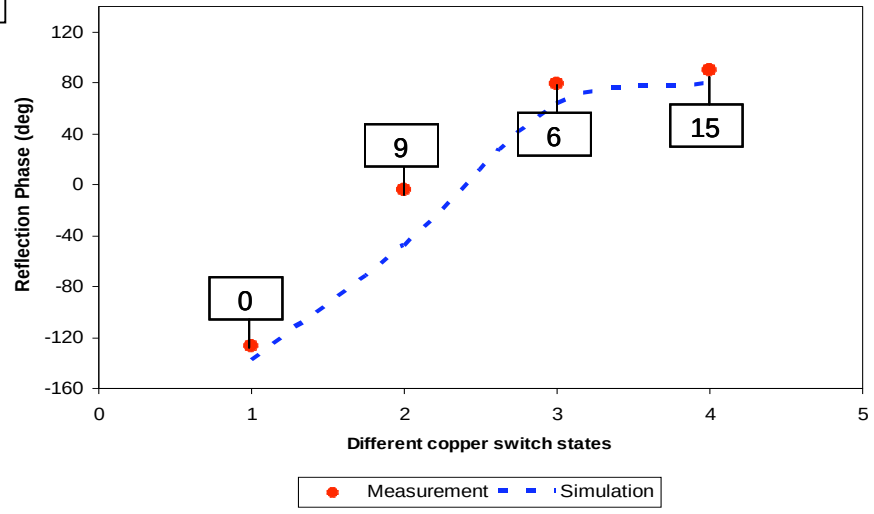

Wire bonds

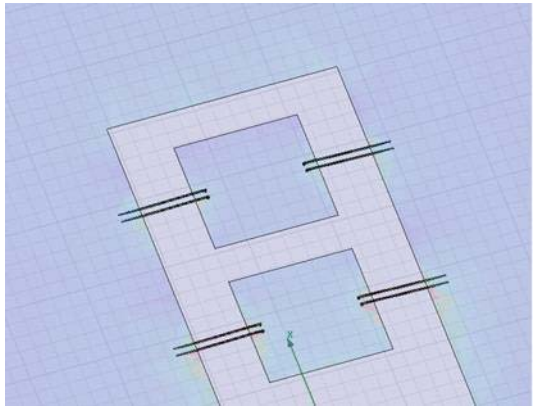

*The active slot length is different for the wire bond case and the currents are concentrated on the wire bonds.

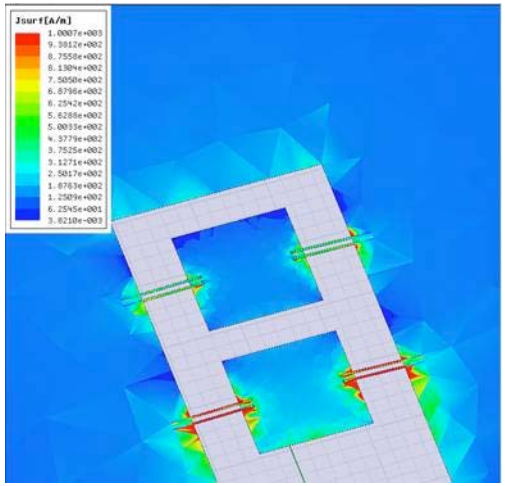

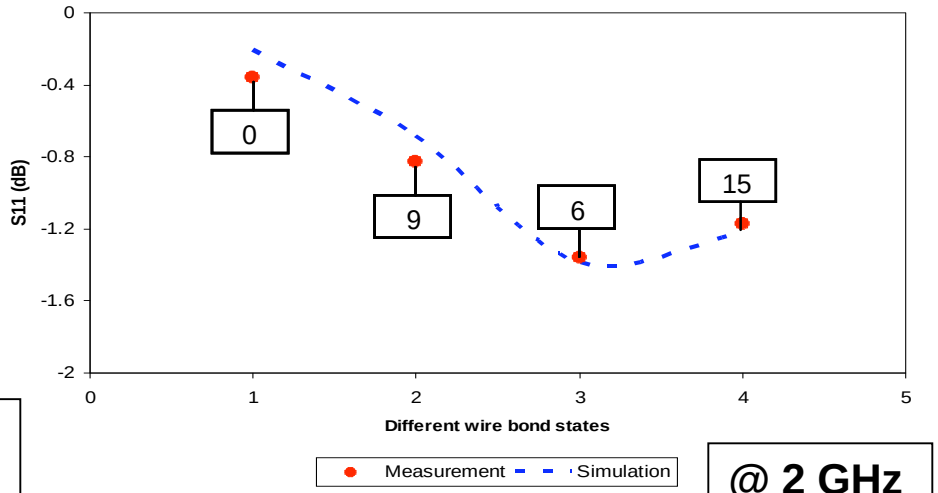

@ 2 GHz

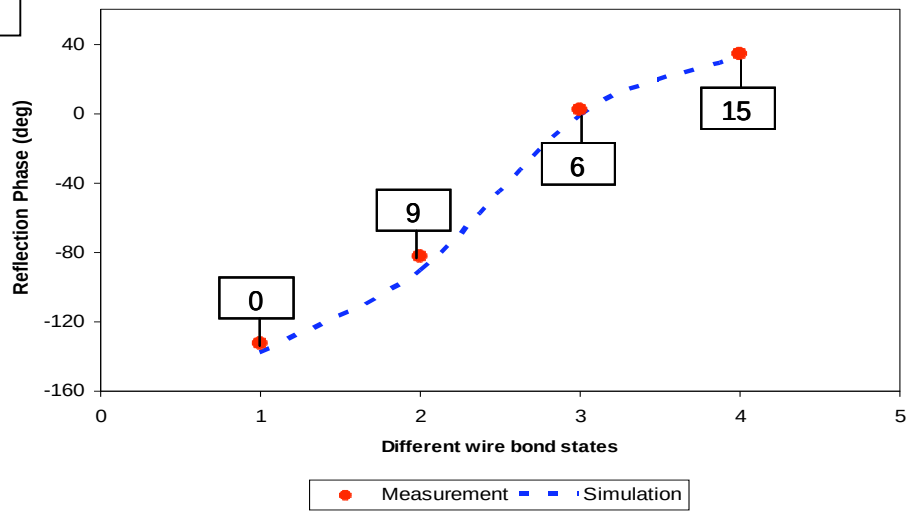

RF MEMS switches (1)

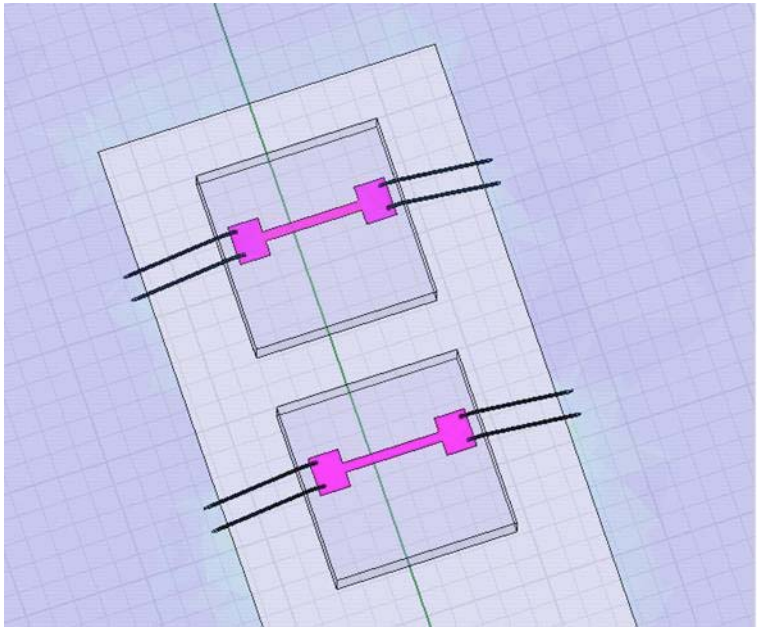

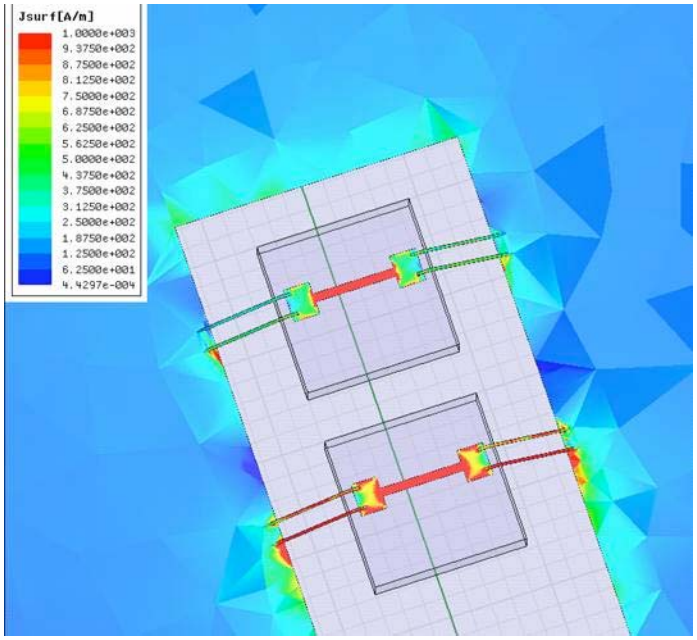

From a black-box point of view, the switch is a microstrip device with pads to access the bias line (gate) and two signal lines (source and drain). These three terminals compose the inputs and outputs into the hermetically sealed switch package, which is fabricated on a grounded silicon substrate. The packaged switch has overall outer dimensions L x W x H = 1.45mm x 1.45mm x 0.25mm.

RF MEMS switches (2)

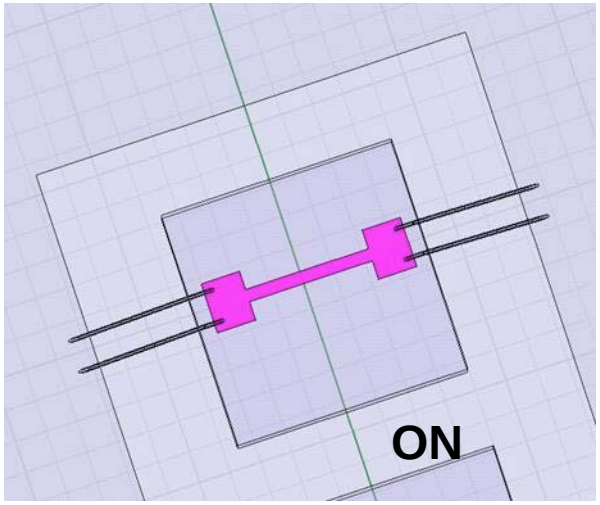

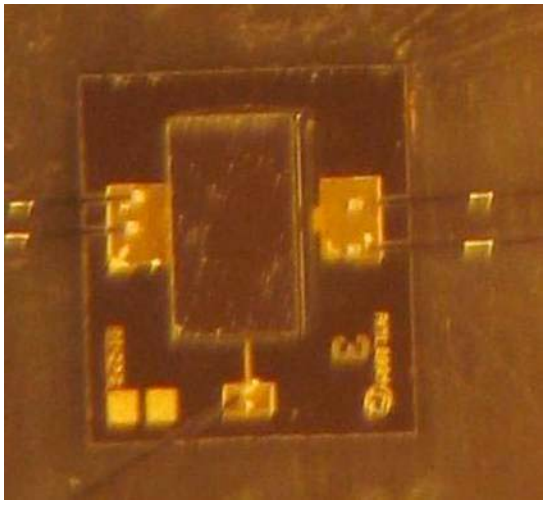

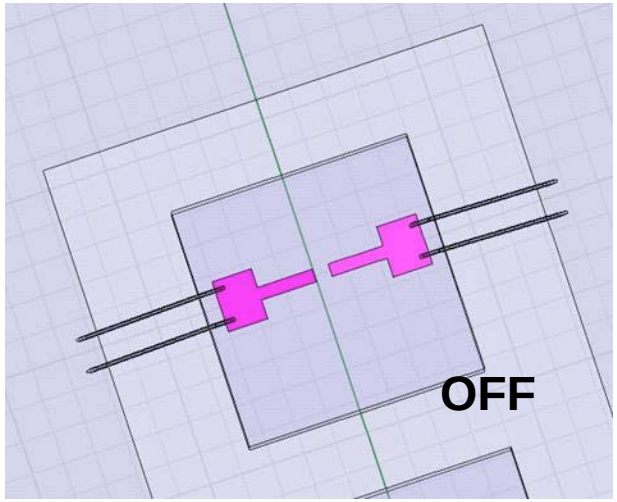

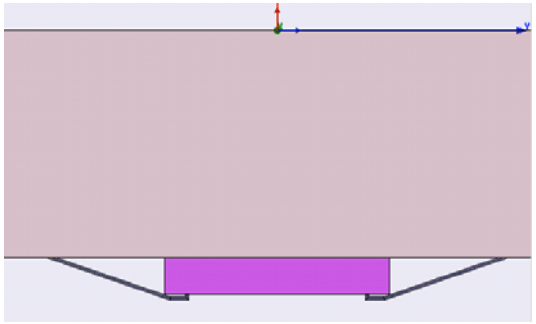

**The effect of gate terminal was studied and it did not have any effect on the phase.

S11 magnitude - RF MEMS switches

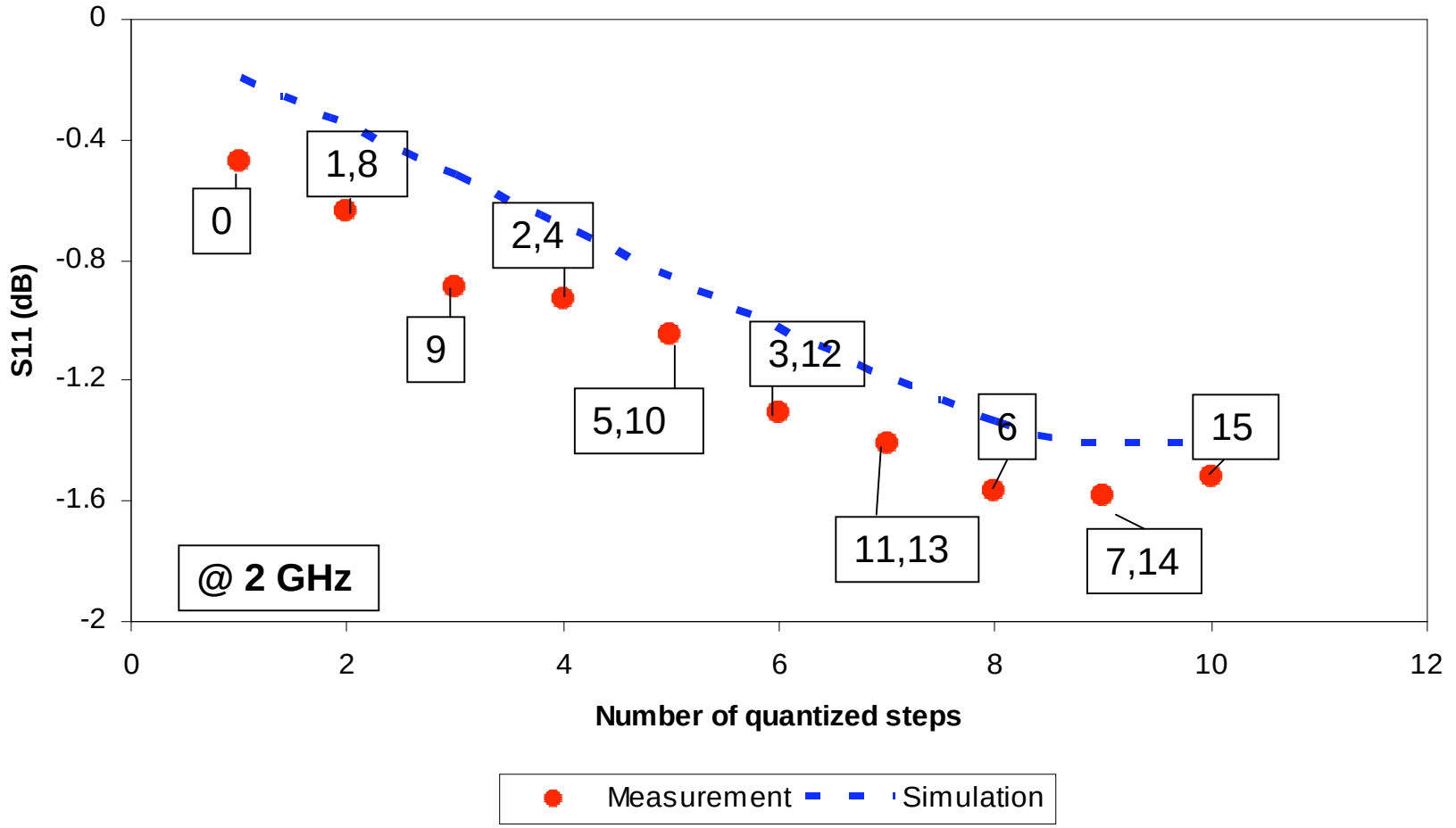

S11 phase - RF MEMS switches

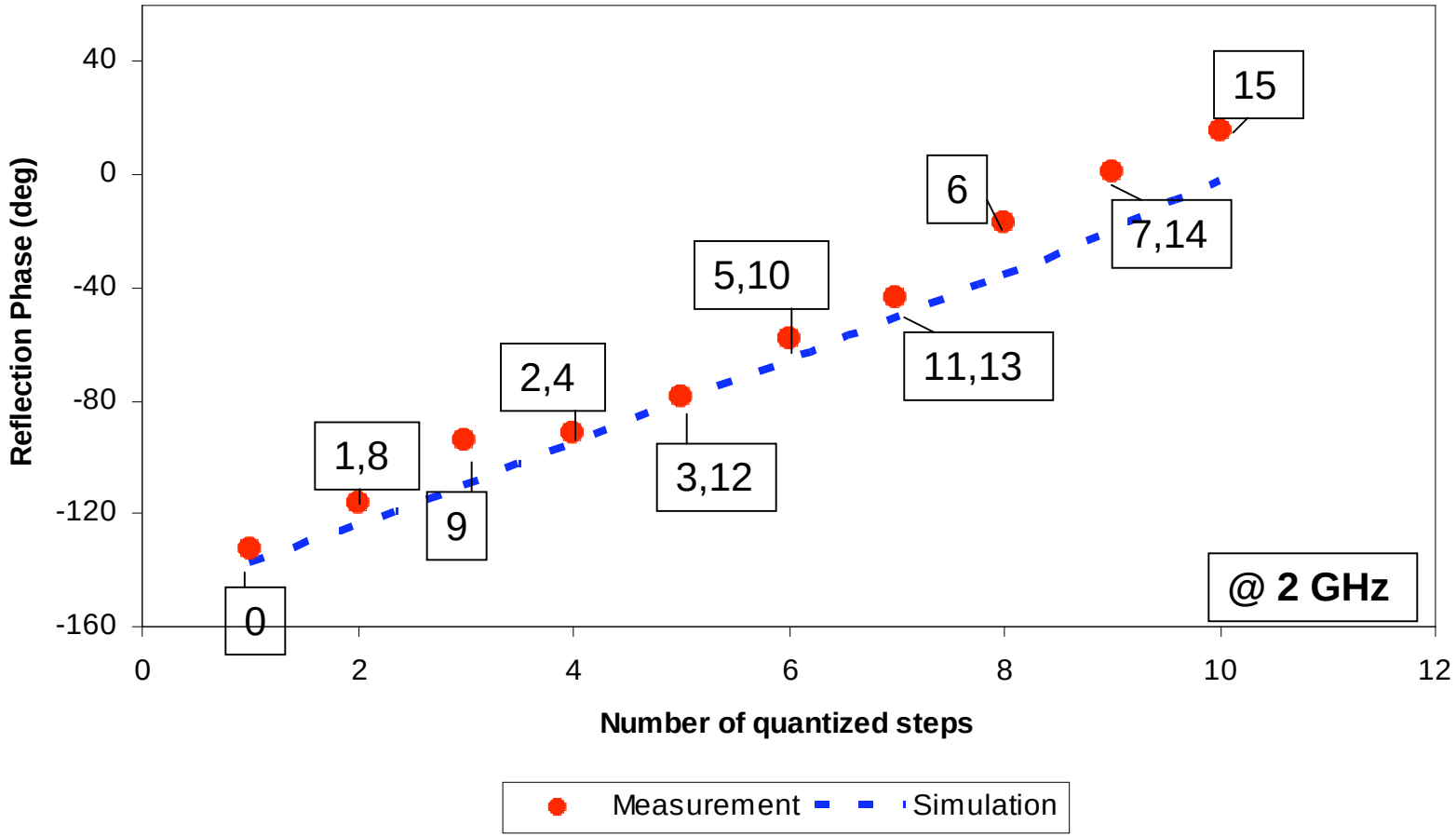

Conclusions

- Three methods for real time surface determination were presented
  - The subreflector probe sampling was determined to be the simplest and a verification experiment is planned
- Analytically, it was determined that a reflectarray subreflector can compensate for main reflector distortion and a verification experiment is also planned
- The optimum patch configuration for integrating MEMS switches was selected
- Using a waveguide simulation experiment, it was successfully demonstrated that MEMS switches integrated into a reflectarray can be used to vary the phase of the reflected field